CHALMERS
UNIVERSITY OF TECHNOLOGY

Construction and initial testing of a lab-scale Chemical Looping system

Master's thesis in the Masters Degree Programme,
Sustainable Energy Systems

ROBERT LARSÉN

Department of Chemical & Biological Engineering
CHALMERS UNIVERSITY OF TECHNOLOGY
Gothenburg, Sweden 2014
This work was performed at the University of Utah, The Institute for Clean and Secure Energy

Construction and initial testing of a lab-scale Chemical Looping system

ROBERT LARSÉN

Supervisor:	Assoc. Prof. Kevin J. Whitty
Examiner:	Assoc. Prof. Henrik Leion

Department of Chemical & Biological Engineering
CHALMERS UNIVERSITY OF TECHNOLOGY
Göteborg, Sweden 2014

Construction and initial testing of a lab-scale Chemical Looping system

ROBERT LARSÉN

Department of Chemical & Biological Engineering
Chalmers University of Technology
SE-412 96 Göteborg
Sweden
Telephone + 46 (0)31-772 1000

This work was performed at the University of Utah, United States of America,
The Institute for Clean and Secure Energy

Cover:
The chemical looping system built in this thesis; see section 6 for design description.

Division of Energy and Materials
Göteborg, Sweden 2014

Acknowledgment

The author wish to acknowledge the supervisor at the University of Utah, Kevin J. Whitty for his support and guidance. PhD student Matthew Hamilton was another helpful source of knowledge. Dana Overacker, Sean Patterson and Shalauna Thompson are acknowledged for their assistance in constructing the system. The metal shop and the chemistry machine shop at the University of Utah have the author's gratitude for their fast and fine work. Finally Åforsk have the author's appreciation for their economic funding of the time in the United States of America.

Construction and initial testing of a lab-scale Chemical Looping system

ROBERT LARSÉN

Department of Chemical & Biological Engineering

Chalmers University of Technology

ABSTRACT

The emission of carbon dioxide is part of the reason why the average temperature on earth is increasing. These emissions are to some extent due to the combustion of fossil fuels and research on means to reduce them is ongoing in several places. The technology that is studied in this thesis is Chemical Looping with Oxygen Uncoupling (CLOU) which is very similar to Chemical Looping Combustion (CLC). Both these technologies use metal oxides (oxygen carriers) to transport oxygen from one reactor to another and this oxidizes fuel. In this way the flue gas is not diluted by the large amount of nitrogen in air but instead it only consists of carbon dioxide and water.

This study presents how a lab-scale chemical looping system is designed and built. The system will later on mainly be run as a CLOU-system but using it for CLC will also be possible and will be a steppingstone before running it as CLOU. When the system was built cold tests were performed to ensure circulation and later on determine the circulation rate during cold conditions.

The design was made in such a way that each part could easily be disconnected in case of redesigning, cleaning or repairing. When the system was built circulation was achieved after additional gas jets were added to the inlets to both the air reactor and the fuel reactor. The length of the standpipe above the upper loop seal was increased from that of the original design due to that the particle level in this pipe went into the cyclone. The circulation rate was shown to increase when the mass of bed material in the air reactor was increased. It was also shown that it increased with increasing flow through the air reactor but it also increased with increased flow through the fuel reactor. The maximum circulation rate that was achieved was around 5 kg/min (11.0 lbs/min).

Keywords: CCS, CLC, CLOU, design, construction, initial testing

Table of contents

Nomenclature

A	Area, m^2
C_D	Orifice coefficient, 0.8
CFH	Cubic Feet per Hour
C_1	Empirical constant, 27.2
C_2	Empirical constant, 0.0408
d	Diameter, m
g	Gravitational acceleration constant, 9.81 m/s^2
h	Height, mm or "
ID	Inner diameter, mm or "
LPM	Litres per minute
OD	Outer diameter, mm or "
P	Pressure, Pa
S	Standard
U	Velocity, m/s
Z	Height, m
"	Inch

Greek letters

ϵ	Bed porosity
μ	Viscosity, Pas
ρ	Density, kg/m^3

Index

b	Bubble
g	Gas
mf	Minimum fluidization
or	Orifice
p	Particle
t	Terminal
x	Cross-sectional
0	Superficial

Dimensionless numbers

Ar	Archimedes number
Re	Reynolds number

Abbreviations

AR	Air Reactor

CCS	Carbon Capture and Storage
CLC	Chemical Looping Combustion
CLOU	Chemical Looping with Oxygen Uncoupling
FR	Fuel Reactor

1. Introduction

Today's widespread usage of fossil fuels results in that large quantities of carbon dioxide (CO_2) are emitted. Since CO_2 is a greenhouse gas it contributes to the increasing temperature on Earth which may have long term consequences [1] [2]. Several ways of reducing the CO_2 emissions have been suggested, for example by implementing Carbon Capture and Storage (CCS). In CCS the CO_2 is collected from incineration in different ways and stored in for example salt water aquifers or depleted oil reservoirs [3]. There are several ways of achieving a pure stream of CO_2; oxyfuel, post combustion and pre-combustion are those alternatives that are the most developed. This thesis on the other hand is focusing on two other technologies called Chemical Looping Combustion (CLC) and Chemical Looping with Oxygen Uncoupling (CLOU). Both these technologies have the advantage that their energy penalty is lower than for the three more developed technologies [4]. The lower energy penalty is due to that the other three technologies require separation of gases which is energy intensive.

2. Background

In this section the basics of CLC and CLOU will be described as well as some essential knowledge about fluidization since the examined chemical looping system relies on the technology. Different kinds of oxygen carriers and an overview of some existing CLC and CLOU system are also presented. Finally a short review of what is done in the field of chemical looping in the United States of America is presented.

2.1. Chemical Looping Combustion

CLC is a technology that uses particles called oxygen carriers to transport oxygen from one fluidized bed to another [5]. A visual presentation of the technology can be seen in Figure 1. Air enters one of the two fluidized beds as fluidization agent, this reactor is called air reactor (AR). In this reactor the oxygen carrier is oxidized and then transported into the second fluidized bed. The second reactor is called the fuel reactor (FR) and here fuel is added, the fuel reacts with the oxygen carrier from the air reactor and reduces it. In this way the flue gas from the fuel reactor only consists of steam and CO_2. When the oxygen carrier is reduced and the fuel is oxidized heat is released due to the energy content in the fuel. Even though heat is released in the system as whole the reaction may be endothermic in the fuel reactor depending on which oxygen carrier and which fuel that is used [6]. Heat is on the other hand always released in the air reactor due to the fact that the oxidation of the oxygen carrier is an exothermic reaction. The fuel reactor is fluidized by either CO_2 or steam to avoid the need for separation of other compounds. Several oxygen carriers have been investigated in previous work and a short description of some of them is given in section 2.4. An example of the oxidation and reduction in CLC can be seen in reaction 1 and 2 below [7]. In the reactions Me_xO_y represents the oxidized oxygen carrier.

Reaction 1

$$(2n+m)Me_xO_{y-1} + \left(n+\frac{1}{2}m\right)O_2 \rightarrow (2n+m)Me_xO_y$$

Reaction 2

$$(2n+m)Me_xO_y + C_nH_{2m} \rightarrow (2n+m)Me_xO_{y-1} + mH_2O + nCO_2$$

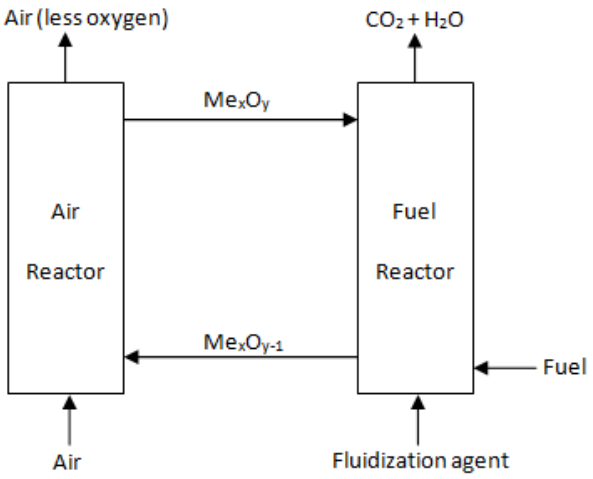

Figure 1. The arrangement of a Chemical Looping Combustion reactor containing two fluidized beds.

A disadvantage with CLC is that solid fuels need to be gasified in order to use them in the CLC process [8]. The reason for this is that since the oxygen is bound to the oxygen

carrier in a solid state the reaction with a solid fuel is very slow. If on the other hand the fuel is gasified there will be a reaction between a solid phase and a gaseous phase, which implies faster reactions.

2.2. Chemical Looping with Oxygen Uncoupling

CLOU also use two fluidized beds but differs since it uses an oxygen carrier that release oxygen as O_2 once it enters the fuel reactor [9]. This gaseous oxygen can thereafter react with the fuel and therefore no gasification of solid fuel is needed, which results in that the fuel conversion is magnitudes faster compared to a conventional CLC-process. Because the reactions are faster not as much oxygen carrier material is needed in CLOU-systems which can reduce the size of the reactors [9]. This of course also lowers the construction and running cost since smaller reactors have lower material cost and less oxygen carriers means that if they break not as much needs to be replaced. Given that the CLOU oxygen carrier need to have the ability to release gaseous oxygen only a few alternatives have been found. The most promising ones are Mn_2O_3/Mn_3O_4 and CuO/Cu_2O [10]. The oxygen carriers are reduced in the fuel reactor since the partial pressure of oxygen is lower in the fuel reactor than in the air reactor which makes the oxygen carrier release its oxygen [11]. The equilibrium partial pressure as a function of the temperature for Mn_2O_3/Mn_3O_4 and CuO/Cu_2O but also Co_3O_4/CoO can be seen in Figure 2 [8].

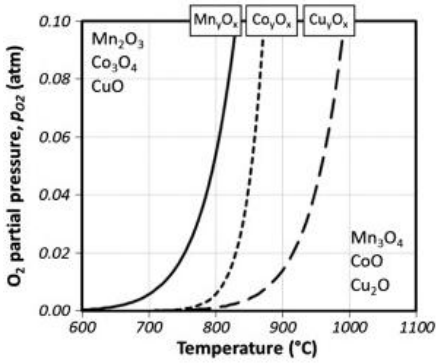

Figure 2. The equilibrium partial pressure for the three oxygen carriers; Mn_2O_3/Mn_3O_4, Co_3O_4/CoO and CuO/Cu_2O.

In a chemical looping process, in this case CLC and CLOU, it is important to ensure that the gases in the respective reactor do not follow the particles to the other reactor. This is important since such slip of gas would contaminate the pure stream of CO_2 or reduce capture efficiency. The separation is done by placing loop seals after the outlets of the reactors before the particles are lead to the inlet of the other reactor. These loop seals ensure that no gas is flowing into the other reactor due to pressure difference [12].

2.3. Fluidized beds

Fluidized beds are achieved by letting a gas or liquid, also called fluidization agent, flow upwards through a bed of particles [13]. The velocity of the liquid or gas needs to be high enough to ensure that the pressure drop over a section is equal to the weight of particles and fluidization agent in that section. At this velocity the particles gets suspended and the solid phase particles obtain physical properties recalling those of fluids, hence the name fluidization. Depending on the fluidization agents velocity different kind of beds will occur. These are, in order of increased velocity; packed bed, bubbling bed, turbulent bed, fast bed and transport bed [14]. In this thesis the setup will consist of a bubbling bed as a fuel reactor and an air reactor with large cross sectional

area in the bottom that after some height is reduced, see Figure 3, section 5. This setup will result in that a bubbling bed will be achieved in the bottom and at least a fast bed in the narrower part. This narrow part will be a riser where the particles are transported to the fuel reactor. The particles will be transported into the fuel reactor since the volumetric flow of gas will be the same in the smaller part as in the wider bottom part. This will result in that the gas velocity in the riser will be larger than in the bottom bubbling bed. The velocity at which a bed is starting to become fluidized is called the minimum fluidization velocity and can be calculated as [14]:

$$U_{mf} = \frac{Re_{mf} * \mu_g}{d_p * \rho_g} \qquad \textit{Equation 1}$$

in which Re_{mf} is the Reynolds number for the minimum fluidization velocity, μ_g is the viscosity of the gas flowing through the bed, ρ_g is the density of the gas in the bed and d_p is the particle size. The Reynolds number is given from the Archimedes number and two empirical constants C_1 and C_2 which are 27.2 and 0.0408 respectively.

$$Re_{mf} = (C_1^2 + C_2 * Ar)^{\frac{1}{2}} - C_1 \qquad \textit{Equation 2}$$

The Archimedes number can be calculated from material data:

$$Ar = \frac{\rho_g * (\rho_p - \rho_g) * g * d_p^3}{\mu_g^2} \qquad \textit{Equation 3}$$

where ρ_p is the particle density and g is the gravitational acceleration.

An example of the standard gas velocity for a bubbling bed with oxygen carriers is 0.5-2.5 m/s and 4-6 m/s for a transport bed [14]. Note that these velocities are examples and that they are dependent on properties such as; bed temperature and pressure, particle size and shape, etcetera which is implied in equations 1 through 3. In a bubbling bed the fluidization agent has such a velocity that bubbles are formed in the bed. In the transition between bubbling bed and fast bed the terminal velocity is an important factor. The terminal velocity is the velocity at which the buoyancy and drag force equals the gravitational force of a single particle. If the velocity of the fluidization agent is larger than the terminal velocity the particle will start moving upwards. This velocity sets a limit between when particles will remain in the same reactor, as in a bubbling bed, or if it will be transported away, as in a fast bed. To ensure that no particles are transported away the velocity should be between the minimum fluidization velocity and the terminal velocity [15]. The terminal velocity can be calculated, assuming spherical particles, dependent on the Reynolds number as [14]:

$$U_t = \begin{cases} \frac{Ar * \mu_g}{18 * d_p * \rho_g} & for\ Re < 0.4 \\ \frac{\left[\frac{Ar}{7.5}\right]^{0.666} * \mu_g}{d_p * \rho_g} & for\ 0.4 < Re < 500 \\ \frac{\left[\frac{Ar}{0.33}\right]^{0.5} * \mu_g}{d_p * \rho_g} & for\ 500 < Re \end{cases} \qquad \textit{Equation 4}$$

where the Archimedes number is given according to equation 3. The Reynolds number is in this case defined as:

$$Re = \frac{U_t * d_p * \rho_g}{\mu_g}$$ *Equation 5*

The terminal velocity can with equations 3 through 5 be calculated in an iterative procedure.

In the riser the gas velocity has to be higher than the terminal velocity to ensure oxygen carrier circulation between the reactors. At very high gas velocities the fluidized bed material will be transported upwards separated from each other [15]. When this occurs the bed is called a transport or entrained bed [14]. At such high velocities the mass flow rate of air is up to 20 times higher than the mass flow rate of the particles giving a dispersed particle profile. When an entrained bed is achieved the particles that are fed to the bed will immediately move upwards. If the velocity is reduced the particles will at some point drop down below the feed point and that is called the choking condition, this marks the lower end of a transport bed.

2.4 Oxygen carriers

As previously mentioned, several oxygen carriers have been examined and they all have their advantages and disadvantages. An oxygen carrier is considered good when it has fast oxidation and reduction rates, an ability to fully convert fuel into water and carbon dioxide, is not deactivated by other compounds and is thermally and physically persistent [7]. If an oxygen carrier cannot fully convert the fuel there will be carbon monoxide and hydrogen gas in the outlet. The more carbon monoxide and hydrogen gas there is in the outlet the more energy is lost since the energy in these gases is not utilized. The amount of oxygen an oxygen carrier can transport is also an important factor. Various metal oxides that have been considered as oxygen carriers are based on; copper, iron, manganese, nickel, cobalt and cadmium [16]. In some cases, when the physical properties of the metal oxide are insufficient, they are sintered with an inert material [17]. Another material called ilmenite, which is a natural ore, has also been proven to be a good oxygen carrier [2]. Ilmenite consists of $FeTiO_3$ and its low price is a considerable advantage [18].

Of the metal oxides only a few have the advantage of fully converting the fuel and they are the ones based on copper, iron and manganese [7]. When using copper as oxygen carrier the temperature may need to be reduced due to its low melting point. On the other hand, this might be solved by sintering as previously mentioned.

2.5 Existing plants

Chemical looping combustion is a relatively new technology and research is ongoing in a number of locations around the world. At some locations the research is focused on finding and evaluating possible oxygen carriers while at other places reactor systems have been built and assessed. Most of these reactors use gaseous fuel but a 10 kW-reactor at Chalmers University of Technology, Sweden, and two reactors of 10 kW and 1 kW in Nanjing, China, use solid fuels [19]. At Vienna University of Technology in Austria there is a 140 kW unit and this size is closer to that of future commercial scale plants.

The design and size of the systems varies between different research facilities [19] [20]. In several places the system design consists of a circulating bed as air reactor and a bubbling bed as fuel reactor. This setup can be seen in two 10 kW reactors at Chalmers as well as in a 50 kW unit at Korea Institute of Energy Research (KIER) in South Korea [19]. Another setup is to have both air and fuel reactor as a bubbling bed. The way of

circulating the particles in these cases also varies; for example in a 10 kW unit for the Spanish National Research Council (Consejo Superior de Investigaciones Científicas, CSIC) in Zaragoza, Spain, the particles from the air reactor is lead to a separate riser which uses air to circulate the particles. In another 50 kW system at KIER, which uses bubbling beds as air and fuel reactor, there are risers put on top of each of the reactors to ensure circulation.

At Vienna University of Technology and at Alstom Power Boilers, USA, they use circulating beds for both the air and fuel reactor [20]. A different setup is used in a 10 kW and a 1 kW unit at South-East University in Nanjing where the air reactor is a circulating bed and the fuel reactor is a spouted bed [19]. Also the number of beds can be altered, for example in a project between IFPEN (Institut Français du Pétrole Energies Nouvelles) and TOTAL a 10 kW pilot plant was built which has three bubbling fluidized beds where two works as air reactors in series and the third is the fuel reactor [21]. At Hamburg University of Technology, Germany, a system with a circulating fluidized bed as air reactor and a two-stage bubbling bed as fuel reactor has been built [22].

At the Technical University of Darmstadt, Germany, a reactor with a maximum thermal power of 1 MW has been built and tested [2]. For the initial tests on this reactor ilmenite was used as oxygen carrier and a Colombian coal was used as fuel. The fuel reactor was fluidized by air and steam which of course is not wanted in a later stage.

An even larger reactor is planned by Cenovus Energy Inc. which is a Canadian oil company that has a big need for steam and want to use CLC to cover this need in the future [23]. Their intention is to, in collaboration with Vienna University of Technology and ANDRITZ Energy & Environment GmbH (AE&E), scale a reactor up to a capacity of 10 MW and commercialise it by 2020. They also believe that when this plant is proven successful, plants with a capacity of 50 and even 100 MW will be commercialised fairly rapidly.

2.6 Chemical Looping in the United States of America

Chemical looping processes are studied in several places across the US. At the institute for clean and secure energy at the University of Utah, in Salt Lake City, CLC and CLOU has been studied in several projects [24]. A number of simulations in ASPEN PLUS have been performed as well as some tests of oxygen carriers in a batch reactor [25]. They have also simulated a 300 kW CLOU reactor in Barracuda and are in the midst of building a cold flow model of this reactor [26].

In the state of Kentucky, CLC is studied at two different universities. At the University of Kentucky oxygen carriers that may be used when using solid fuels have been investigated [27]. At the Western Kentucky University both a 10 kW equivalent cold model and a 10 kW hot model of a CLC has been built and operated [4]. Their next stage in the research is to adapt an existing 0.6 MW circulating fluidized bed combustor into a 1 MW CLC reactor.

Oxygen carriers are also studied at Li Research Group on the North Carolina State University [28]. At the University of Connecticut they try to find both good oxygen carrier but also a reactor design that would take advantage of the carrier properties [29].

At Ohio State University (OSU) they study a technology called coal direct chemical looping (CDCL) combustion and they have a reactor with a capacity of 25 kW_{th} that

uses this technology [30]. This technology was developed at OSU and enables a coproduction of heat and hydrogen [31]. At Carnegie Mellon University they use chemical looping to enhance gasification of coal [32]. Using their technology the product gas only consists of hydrogen and methane whilst the carbon dioxide is retrieved at another outlet.

3. Purpose

The aim of this thesis is to design and build a lab scale chemical looping system and make first measurements on it. The fuel reactor will be a modification of an old gasifier built as a part of a master thesis in 2011 [33].

The measurements will be performed by using aluminium oxide as particles and air as fluidization agent in all parts without heating the system. During these cold conditions circulation will be ensured and the circulation rate will be examined. Note that during the design phase a hot system will be considered.

This lab scale reactor will be used in future studies at the University of Utah in Salt Lake City for further investigation of CLC and ultimately CLOU.

4. Boundaries

The construction will be restricted to one bubbling fluidized bed as fuel reactor and a bubbling fluidized bed with a riser as air reactor. There will be loop seals between the reactors to ensure no slip of gases.

The research will be limited to cold tests of the equipment using aluminium oxide, AlO_3, as particles and fluidizing all parts with air. This mean that further studies running the equipment as CLC and finally CLOU will not be performed within this thesis.

5. Method

The reactor setup that is built will consist of one bubbling fluidized bed as the fuel reactor and one bubbling fluidized bed with a riser as the air reactor, see Figure 3. The air reactor will be connected to a cyclone and after that to a loop seal before entering the fuel reactor. The oxygen carriers leaving the fuel reactor, through the middle pipe, will go through another loop seal before being lead back into the air reactor.

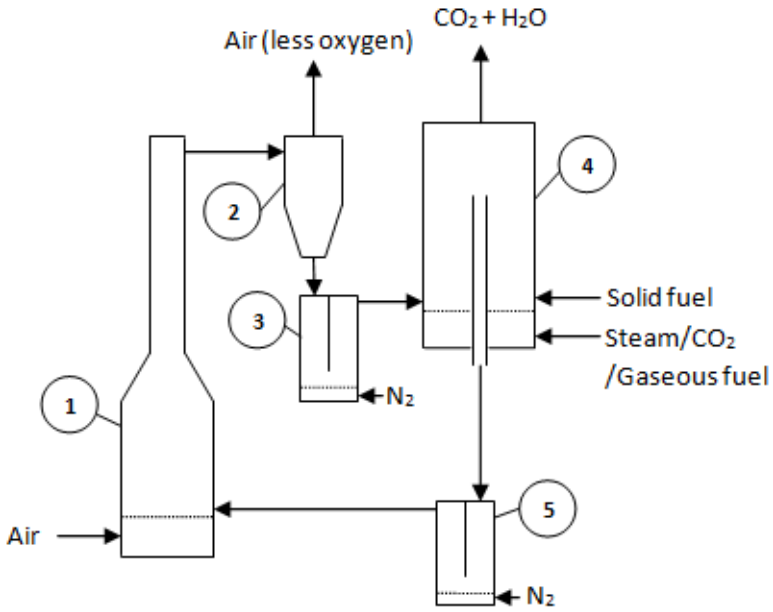

Figure 3. A simple drawing of the parts in the chemical looping system that is being built. Where; 1 is the air reactor, 2 a cyclone, 3 a loop seal, 4 the fuel reactor and 5 another loop seal.

After the system has been built according to Figure 3 the measurements will commence. The initial testing consists of making sure that circulation of particles is achieved. This is done by running the system at room temperature and swapping some of the tubing out for transparent hose and looking for build-up of particles in the different parts.

The next step is to measure the circulation rate of the system. This will be done by swapping the tube from the cyclone to the upper loop seal out for a transparent hose. The air to the loop seal is thereafter shut off and the time it takes to fill up the hose with a certain height of particles will give an indication of the circulation rate. How the circulation rate is affected by the following three cases will be studied:

- 5.85 kg (12.9 lbs) of particles in the AR and varying the flow in the AR
- 7.31 kg (16.1 lbs) of particles in the AR and varying the flow in the AR
- 7.31 kg (16.1 lbs) of particles in the AR and varying the flow in the FR

The particles that will be used at this stage of the tests are particles of aluminium oxide sand. The bulk density of the particles as well as their size distribution was determined through weighing measured volumes and sieving them respectively. The bulk density of the particles was determined to 1700 kg/m^3 and the size distribution can be seen in Table 1.

Table 1. Size distribution of the aluminium oxide used in the initial tests.

Size	Percentage
850 μm < Size	0.82%
425 μm < Size < 850 μm	1.43%
250 μm < Size < 425 μm	2.78%
180 μm < Size < 250 μm	79.53%
Size < 180 μm	15.45%

6. Designing the chemical looping system

In the following section the design of the chemical looping system is explained and clarified. Throughout the design the software SolidWorks was used to draw all parts in 3D. This simplified the design process since it gave a visual representation of what was going to be built and how it came together. The finished drawing of the system from SolidWorks can be seen in Figure 4. For more detailed drawings of the different parts see Appendix A and for a list of building material see Appendix B. The parts that are described are; the fuel reactor, the air reactor and the loop seals.

Since the project was performed in the United States of America the design was done in United States customary units. To simplify for readers the units have been converted into the metric system with the design units in parenthesis. Note that in all drawings the dimensions are in inches. The cyclone was an old part which had suitable dimensions for the separation needed and was therefore reused in this project. The cyclone consists of a 124 mm (4.88") OD and 111 mm (4.38") ID tube which is 229 mm (9") high and a cone-shaped part which reduces the size down to 38.1 mm (1.5") with the same wall thickness and is 229 mm (9") tall. When designing the system the possibility of having each part separable from the system was desirable in case redesigning, cleaning or repairing is needed. All tubing between the different parts is tubing of 38.1 mm (1.5") outer diameter (OD) and 34.8 mm (1.37") inner diameter (ID). The only tubing that does not have these dimensions is the tube between the fuel reactor and the lower loop seal (parts number 4 and 5 in Figure 4 respectively) which instead has 25.4 mm (1") OD and 22.1 mm (0.87") ID. The reason for this is that there is not enough space for a wider tube coming up through the bed in the fuel reactor due to the bubble caps on the old gasifiers distributor plate. Mounting brackets (one for the fuel reactor, one for each of the loop seals, one for the cyclone and one for the solid fuel feeder) have also been designed and built to keep the centre-line for all parts 356 mm (14") from the wall. These brackets will however not be described further. The air reactor is standing on the floor on three feet which can be altered in height in case some small adjustments are necessary.

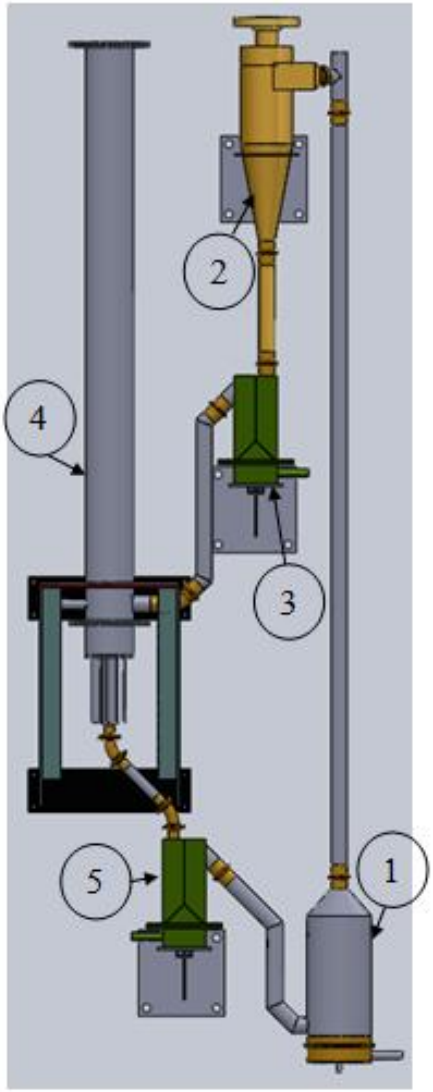

Figure 4. The final design of the system. The numbers represent the following parts; 1. Air reactor, 2. Cyclone, 3. Loop seal, 4. Fuel reactor, 5. Loop seal

6.1 Fuel reactor

As previously mentioned the fuel reactor was made by modifying an old gasifier. The modification that was necessary was that an extra piece was added between the plenum and the reactor body. This extra piece was made to ensure that both the solid fuel and particles coming from the air reactor can enter the bottom of the reactor from opposite sides. The OD and ID of the extra piece were made to be the same as the existing gasifier and their dimensions can be seen in Table 2. The reason for putting the fuel inlet in the bottom is to make certain that the solid fuel have enough time to react. If the time is too short the fuel may go out through the top of the fuel reactor as volatiles or follow the metal particles into the air reactor. The particles are also added in the bottom to reduce the risk of particles falling straight down the exit pipe sticking up through the bed. For the initial tests the pipe sticking up through the bed will be tall enough to ensure a bed height of 254 mm (10"). Note that the bed height in the fuel reactor can be changed by changing this pipe since it is interchangeable.

Table 2. The dimensions of the old gasifier as well as the additional piece for fuel and particle inlets which together makes the fuel reactor.

	[mm]	["]
OD	114	4.5
ID	102	4
Height gasifier	1270	50
Height extra piece	88.9	3.5
Total FR height	1360	53.5
Bed height	254	10

6.2 Air reactor

This design consists of a bubbling bed with a riser on top to make the particles circulate. The cone-shaped part of the air reactor reduces the diameter of the bubbling bed to that of the riser and is 63.5 mm (2.5") tall. The dimensions of the air reactor parts can be seen in Table 3 and in Figure 5, note that in the figure the dimensions are given in inches.

Table 3. The dimensions of the different part of the air reactor.

	Bubbling bed		Riser	
	[mm]	["]	[mm]	["]
OD	152	6	38.1	1.5
ID	147	5.78	34.8	1.37
Height	305	12	1970	77.5

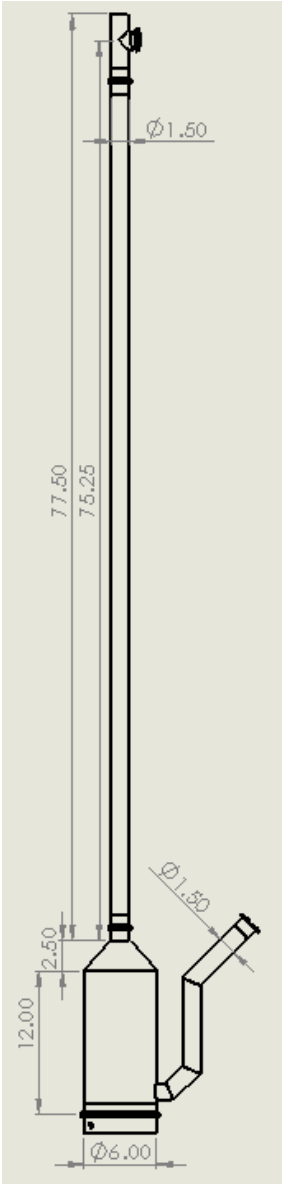

Figure 5. A drawing of the air reactor with the dimensions in inches.

With these dimension the required gas flow can be determined to ensure a bubbling bed in the bottom and at least a fast bed in the riser. The terminal velocity was determined for both the riser and the bubbling bed according to equations 3, 4 and 5. The material data estimated in these calculations can be seen in Table 4, in which the gas properties are taken for air at atmospheric pressure and 900°C. Note that this data is different from the one listed in Table 1 due to the fact that the hot system is meant to run with some sort of copper-based oxygen carrier which has different density than the aluminium oxide in the initial tests [11]. The density of the copper-based oxygen carrier is dependent on how it is manufactured and what material it is sintered to.

Table 4. Material data used in the calculation of the terminal velocity according to equations (3-5).

d_p	200 μm
ρ_p	2600 kg/m^3
ρ_g	0.3 kg/m^3
μ_g	47*10^{-6} Pas

With both the minimum fluidization and the terminal velocity calculated from equation 1 and 3 through 5 respectively a range of flows for the bottom bubbling bed could be determined as can be seen in Figure 6. In this figure the gas velocity in the bottom part is plotted as a function of the volumetric flow.

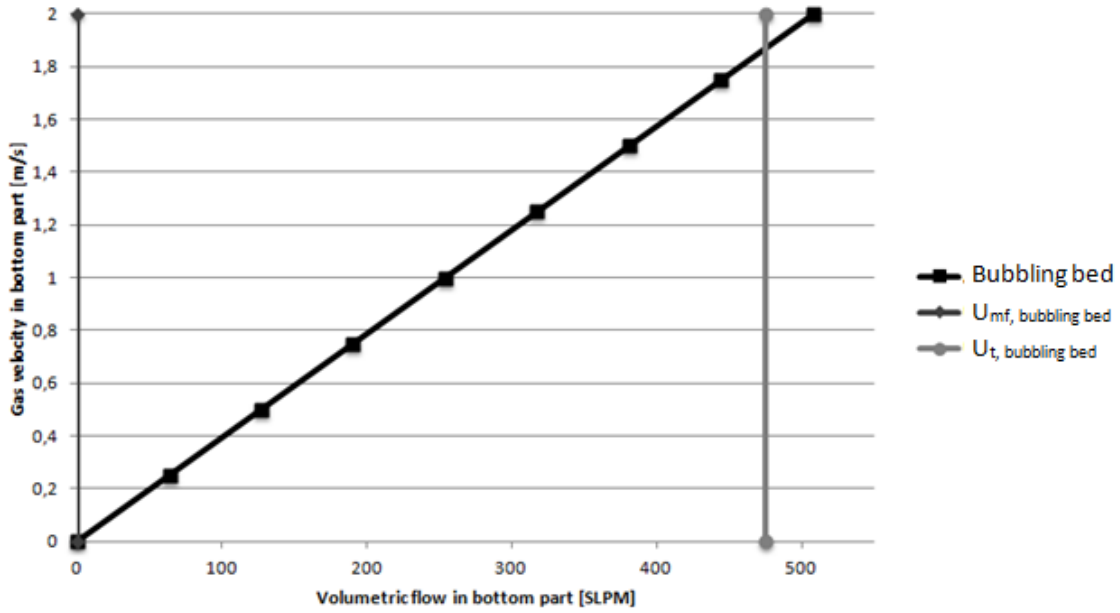

Figure 6. The flow rate and the corresponding superficial velocity in the bubbling bed in the bottom of the air reactor. At velocities higher than the terminal velocity, u_t, the bottom part is no longer guaranteed to be a bubbling bed but might transfer into a transport bed.

The terminal velocity was also calculated for the riser since a velocity higher than the terminal velocity is needed in this section in order to get upward transportation of particles. This showed that the terminal velocity will not be reached for the full range in Figure 6. Instead the terminal velocity of the riser will set a new lower limit to the volumetric flow. The result can be seen in Figure 7 where the velocity for both the riser and bottom part can be seen as a function of the volumetric flow in the bottom part.

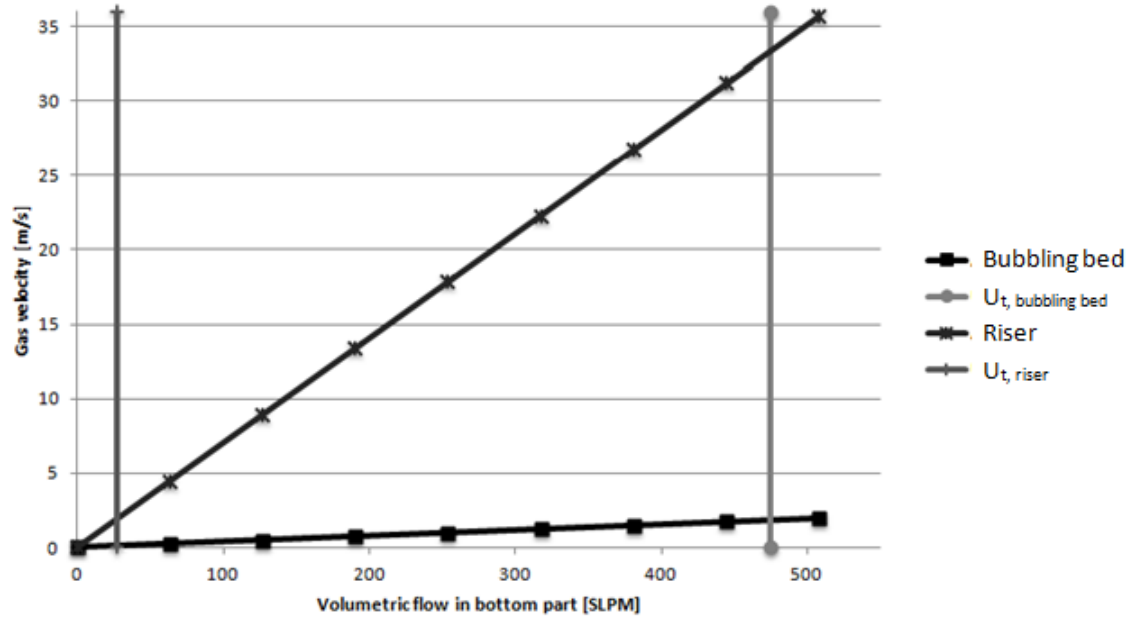

Figure 7. The volumetric flow and the superficial velocity in the bottom bubbling bed as well as the resulting superficial velocity in the riser.

Since the velocity range in the bubbling bed is hard to see in Figure 7 due to the large velocity difference in the different parts a simplified view is presented in Figure 8. In Figure 8 the gas velocity in the bottom part is plotted as a function of the volumetric flow. The range is here limited by the terminal velocity in the riser at the lower end and the terminal velocity in the bottom part at the higher end.

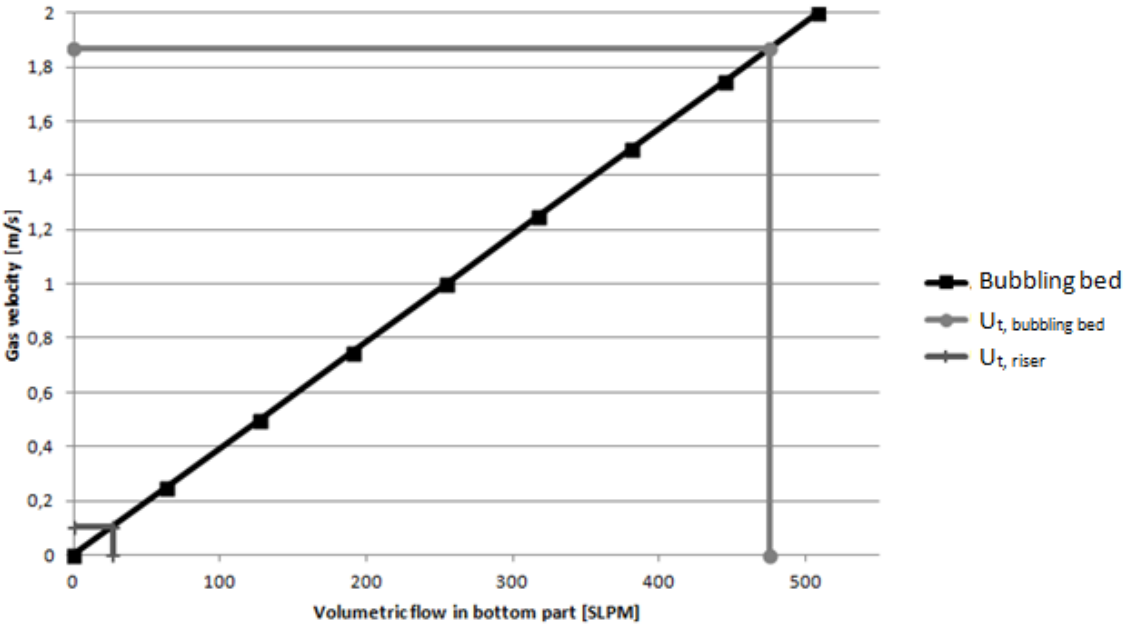

Figure 8. The final range of the superficial velocity and volumetric flow in the bubbling bed that ensures transport bed in the riser.

In Figure 8 the superficial velocity and air flow ranges from 0.105 m/s to 1.87 m/s and 26.7 SLPM (56.5 SCFH) to 475 SLPM (1010 SCFH). The lower limit is because a

velocity greater than the terminal velocity is needed in the riser and the higher limit is to not exceed the terminal velocity in the bottom part.

The air reactor plenum was designed to have 36 holes with a diameter of 1.59 mm (0.0625") and the hole pattern can be seen in Figure 9. This number of holes, as well as the size, was determined to ensure sufficient pressure drop over the distributor plate in a similar way as for the loop seals in section 6.3.2. Since the hole size is bigger than the particle size a stainless steel screen was welded to the top of the distributor plate to prevent the particles from dropping down into the plenum. If particles fall down into the plenum they may have an eroding effect when they are blasted back through the orifices of the distributor plate [34].

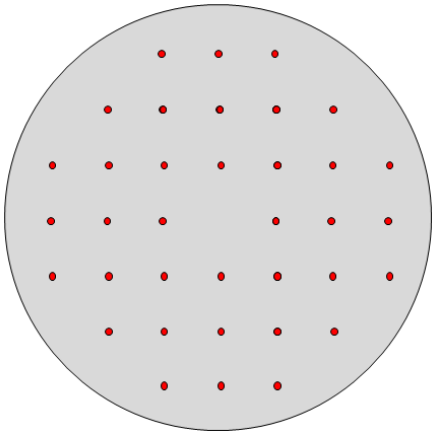

Figure 9. Air reactor distributor plate hole pattern where each hole is 1.59 mm (0.0625'').

6.3 Loop seals

In this section the design of the loop seals and their distributor plates are described. The design of the two loop seals are the same as well as their distributor plates except that the inlet to the lower loop seal (number 5 in Figure 4) is 25.4 mm (1") OD compared to the 38.1 mm (1.5") OD for the upper loop seal (number 3 in Figure 4).

6.3.1 Loop seal design

A square design was used for the loop seals to simplify the construction of distributor plate and the length of the sides was chosen to be close to that of the OD of the tubing connecting different parts. They were built by welding two square tubes together and removing the wall between them by the bottom end. The square tubing used had a side length of 63.5 mm (2.5") outside and 57.2 mm (2.25") inside. This gave a total loop seal size of 127 mm (5") by 63.5 mm (2.5") outside and 114 mm (4.5") by 57.2 mm (2.25") inside. The height of the outlet is supposed to be around 2.5 times the length of the side in the loop seal [35]. In this project a height of 140 mm (5.5") was chosen which is 2 times the side length.

A drawing of the loop seals can be seen in Figure 10, in which the dimensions are given in inches. As can be seen in the figure there is a flange at the bottom of the loop seal to be able to bolt it to the plenum. It is also obvious that the loop seal can be removed from the system easily due to the two connectors, one on each of the inlet and outlet.

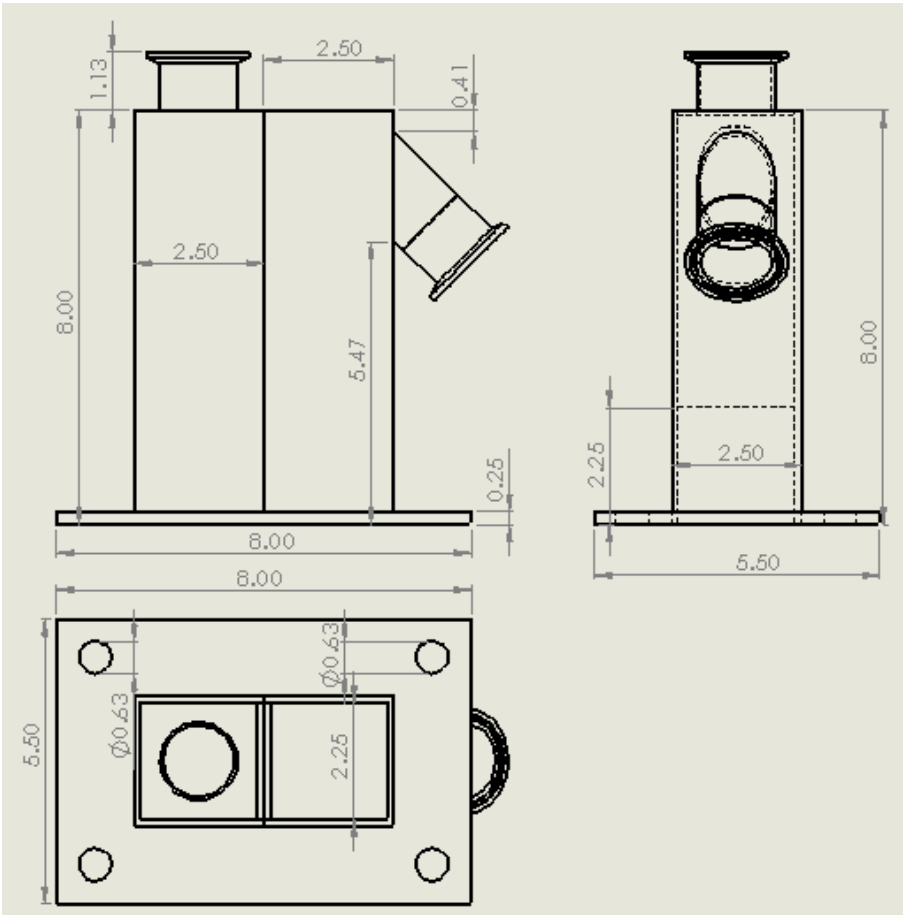

Figure 10. The finished loop seal design with a flange on the bottom to be able to bolt it to the plenum.

6.3.2 Distributor plate

When designing the loop seals distributor plates it is important to ensure sufficient pressure drop across the distributor plate to reduce the risk of uneven fluidization. The pressure drop is dependent on the number of holes and the size of the holes in the plate. This dependence can be seen in the equations below [34]. The pressure drop across a fluidized bed is calculated as:

$$\Delta P_{bed} = \rho_p * (1 - \epsilon) * h * g \qquad \textit{Equation 6}$$

where ρ_p is the same as in Table 4, ϵ is the bed porosity and h is the height of the bed which in this project is 0.14 m (5.5"). The bed porosity can be estimated by:

$$\epsilon = \frac{U_0 + 1}{U_0 + 2} \qquad \textit{Equation 7}$$

in which U_0 is the superficial velocity. The superficial velocity is set slightly above the minimum fluidization velocity which can be calculated with equation 1 and the material data provided in Table 4. The minimum fluidization velocity was calculated to 0.016 m/s and the superficial velocity, U_0, was therefore set to 0.05 m/s to guarantee fluidization of the bed.

With these things known the pressure drop of bed was calculated to 1740 Pa. The pressure drop over the plate should be at least 20% of the total pressure drop over the bed and plate to ensure even fluidization [34].

$$\Delta P_{plate} = \frac{0.2 * \Delta P_{bed}}{1 - 0.2}$$ *Equation 8*

This results in a minimum acceptable pressure drop over the distribution plate of 435 Pa. Now the number of holes, N, as well as the diameter of the holes, d_{or}, can be decided from equation 9:

$$N * d_{or}^2 = \frac{U_0 * \rho_g * A_x * 4}{\pi * U_{or} * \rho_{g,or}}$$ *Equation 9*

where A_x is the cross sectional area of the bed which is 0.0069 m^2 for the loop seal, $\rho_{g,or}$ is the density of the gas in the orifices estimated to 0.52 kg/m^3 (density of air at a preheated temperature of approximately 400°C) and U_{or} is the velocity through the orifices, which can be calculated as [34]:

$$U_{or} = C_D * \left(2 * \frac{\Delta P_{plate}}{\rho_{g,or}}\right)^{\frac{1}{2}}$$ *Equation 10*

In equation 10, C_D is the orifice coefficient which can be approximated to 0.8. The hole diameter was set to 0.794 mm (0.0313") which was the smallest holes that could be drilled. Since this is also larger than the particle size a stainless steel screen was welded to these distributor plates as well. The number of holes was then decided to six to come close to the minimum pressure drop and still have a significant margin to not risk uneven fluidization. The pressure drop that was achieved with these dimensions was 1820 Pa. This might seem unnecessarily high but this gives a rigid design in which the gas, the temperature of the gas and the particles can be changed without fearing uneven fluidization. The hole pattern was decided to be as in Figure 11 where the two middle holes are beneath the separation wall in order to simplify the transportation of particles.

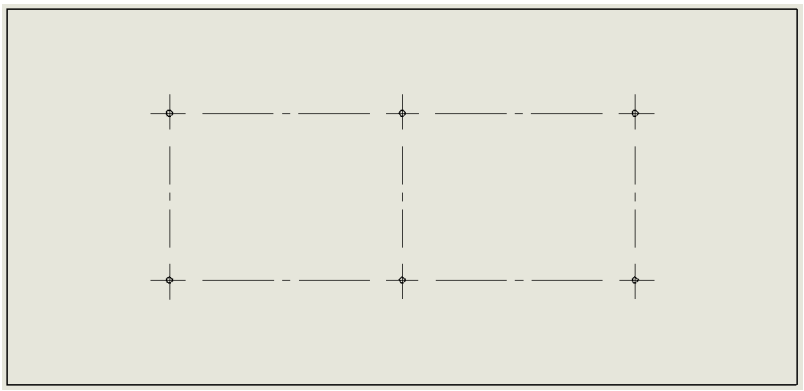

Figure 11. Hole pattern on the loop seal distributor plate. The holes are 0.794 mm (0.0313") in diameter. The middle holes are put underneath the separator wall in the loop seals to improve circulation.

To ensure that the fluidization was not located to one small stream of bubbles the bubble size was calculated. This was done according to equation 11 [14]:

$$d_b = 0.54 * \left(U_0 - U_{mf}\right)^{0.4} * \left(Z + 4 * A_{or}^{\frac{1}{2}}\right)^{0.8} * g^{-0.2}$$ *Equation 11*

where Z is the height at which the bubble size is wanted, this was chosen as 57 mm (2.25") which is the height at which the wall separation starts. A_{or} is the cross-sectional area of the orifices in the distributor plate. This gave a bubble size of 9.3 mm which was

considered large enough for the six holes in the plate. If the bubble size would have been too small more number of holes would have had to be drilled to distribute the gas jets more evenly across the bed.

7. Results and discussion

How circulation was achieved is described in this section and also the results from the circulation tests are presented. The built system can be seen in Figure 12. In this figure a solid fuel feeder has been installed, to the left, as well as a char filter, to the right. On the outside of the FR heaters have been mounted and the tubes leading the flue gas from the FR to the filter have been wrapped with heating tape and insulated. The filter have also been wrapped in heating tape and insulated but since the tests performed in this study were carried out at room temperature this was of no importance. In future studies of CLC and CLOU on the system also the rest of the equipment will be insulated.

Figure 12. The system in reality. To the left a solid fuel feeder has been installed and to the right there is a char filter. On the outside of the fuel reactor heaters have been added.

7.1 Achieving circulation

The flow of gas and the amount of particles in the loop seals were determined by filling them up to a reasonable point and then flow gas through it and physically feel when the particles became fluidized. The flow at which this happened was at 10.2 SLPM (21.7 SCFH) but a more reasonable level for operation was chosen to 12.3 SLPM (26.0 SCFH). The loop seals were thereafter filled up during fluidization to the point where particles started pouring out through the outlet. The following section will henceforth go through the different tests that were run to achieve circulation and the outcome of these tests.

In the first test particles seemed to be circulating, but after some consideration it was noticed that the amount of particles in the FR was too low. This resulted in that the air

flow in the FR was set too high, 91.9 SLPM (195 SCFH), since at high enough velocities particles will drop down the middle tube due to that a fast bed is approached. This error was observed when the lower loop seal was blown out due to the high flow of air inserted in the fuel reactor. The blow-out was noticed when the AR flow was shut off and particles were still falling out from the cyclone. In the search for what could have caused this the top of the FR was taken off and a visual study of the bed at different velocities was performed. It was concluded that the particle level was too low and the velocity of air was too high. The appropriate air flow through the FR was determined to 20.4-30.6 SLPM (43.3-65.0 SCFH).

A new trial was commenced with a flow of 30.6 SLPM (65.0 SCFH) in the FR and a flow of 245 SLPM (520 SCFH) in the AR. At first everything seemed to be working as it should but at one point particles stopped falling out from the cyclone. When trying to figure out what had gone wrong it was discovered that no particles were flowing in to the AR. The system had been plugged in the tube leading to the AR. The first thought was that an additional jet of air might be needed to be inserted in the tube to force the particles into the reactor. When the AR bottom part was drained and taken apart it was notice that the screen welded on top of the distributor plate in order to prevent particles from falling through the holes had been blasted over a couple of holes as can be seen in Figure 13. This was a clear indication that the sheet had not sealed sufficiently and particles had fallen into the plenum. It was also confirmed when the plenum was turned on its end and particles were pouring out of it. The remainder of the holes, the ones not having blasted the screen, were instead plugged with particles. Since most of the holes were plugged this was seen as the reason for why particles were plugging the inlet to the AR and no additional jet was therefore inserted.

Figure 13. The screen welded on top of the distributor plate in the air reactor after some time running the system. The smaller holes are the ones that had been blasted open by particles that had fallen into the plenum. The big hole is a hole cut out in order to be able to drain the bed.

The screen was replaced with the same stainless steel material but the middle big hole was not cut out this time to ensure that particles would not fall in under the screen through this hole. This meant that draining the bed was now impossible since the particles cannot penetrate the screen. This was not considered to be a big issue since if drainage was needed the whole bottom part could be disconnected and the particles could be poured out. Air was again added at the same rates as in the previous test and circulation seemed to be working. The flow through the AR was lowered and after some time it became clear that build-up of particles occurred in the inlet tubes to both the AR and the FR. The flow was increased to the initial level of 245 SLPM (520 SCFH) in order to see if this would remove the built up particles. This was not the case and therefore a gas jet was added to each of the inlets to push the particles into the reactors.

The result of this was tested by not having any gas flowing and trying to fill the reactors from their respective inlets. This of course plugged the inlet tubes. Then air was added through the distributor plates in order to see if that would help remove the plug. It did not help so air was added to the jet, the plug was removed and particles were flowing into the reactors. In other words this solution worked for both the AR and the FR.

At this point it also became clear that the build-up of particles in the standpipe above the upper loop seal was higher than the length of the tube connecting the loop seal to the cyclone. The build-up was expected to some extent but if it reaches up into the cyclone it might affect the cyclones performance or ultimately fill it up completely. To solve this problem the standpipe between the cyclone and the upper loop seal was increased by 518 mm (20.4") and the riser was increased by the same amount in order to make up for this. The previous length of the tube connecting the cyclone to the loop seal was 260 mm (10.25") and the addition increased its length to 779 mm (30.65"). A transparent hose was put between the cyclone and the loop seal to see at what height the particles reached steady state. This height increased with higher flows through the AR but the maximum observed level was around 457 mm (18") into the tube. Since this is almost 200 mm (7.87") more than the original length of the tube it would have resulted in that the cyclone would have been filled with particles to some extent with the previous shorter tube. With this problem solved the system was concluded to circulate.

7.2 Circulation rate

The circulation rate was as previously mentioned measured for three different cases. The data was evaluated by plotting the mean and taking the standard error of the measurements into account which can be seen in Figure 14 through Figure 17. For all the measurements the flow through the loop seals were kept constant at 12.3 SLPM (26.0 SCFH). When the flow through the AR was altered the flow through the FR was kept at 30.6 SLPM (65.0 SCFH) and when the flow in the FR was changed the flow in the AR was kept at 147 SLPM (312 SCFH).

The results for the case with 5.85 kg (12.9 lbs) of particles in the AR can be seen in Figure 14. For each volumetric flow several measurements was done to give more trustworthy results. It is obvious that the circulation rate increases with increasing volumetric flow and seem to be of non-linear dependency. The increased circulation rate with increased volumetric flow is somewhat intuitive since a higher flow result in a higher velocity of the gas and more particles should therefore be dragged along upwards through the riser. The value at 220 SLPM seems a bit odd compared to the other values but the standard error at this point is also comparably large as well, which might suggest that this value is somewhat unreliable. Another reason for why the circulation rate for higher flows might be off is that when the loop seal is turned off the feed of particles to the AR shuts off as well. This results in that the mass of particles in the AR is reduced by as much that is built up in the transparent hose. The amount of particles that was filled up in the transparent hose was increased at higher flows in order to make more accurate measurements. This also meant that more particles were taken from the AR at these flows and ultimately reducing the mass more compared to when doing the tests for the lower flows.

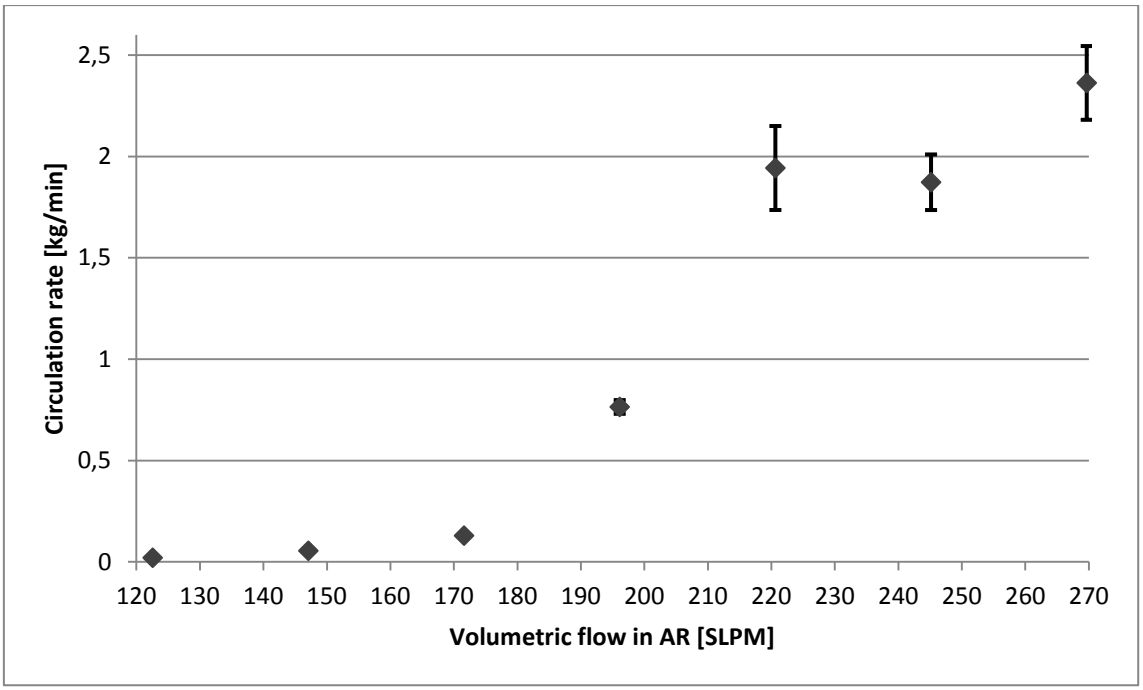

Figure 14. The circulation rate as a function of the volumetric flow in the AR when there is 5.85 kg (12.9 lbs) of particles in it. There seems to be a non-linear dependency between the flow and the circulation rate and the maximum circulation rate was measured to 2.5 kg/min (5.51 lbs/min).

As can be seen in Figure 14 the circulation rate was measured to be as high as 2.5 kg/min (5.51 lbs/min). This value might become even higher at larger flows but this was the maximum value that could be achieved during these tests.

When the mass of the bed in the AR was increased to 7.31 kg (16.1 lbs) the circulation seemed to get a linear relation to the flow rate which is shown in Figure 15. The maximum circulation rate achieved in this case was around 5 kg/min (11.0 lbs/min). When comparing the two different cases with different mass in the AR it is obvious that the circulation rate is larger for the same flow when the bed weight is increased. This can more easily be noticed in Figure 16. The reason for why the circulation rate is larger when there are more particles in the reactor may be due to the fact that the top of the bubbling bed in the AR is closer to the riser and therefore it might be easier for particles to travel up through the riser. Compare this to a case with a very tall bottom section and a low bed; in order for particles to circulate in such a case the terminal velocity have to be breached in the lower section in order to transport the particles up to the riser. When a bed is too low the velocity have to be rather high in the reactor to get good circulation or only the smaller particles will be transported up through the riser since smaller particles have lower terminal velocity.

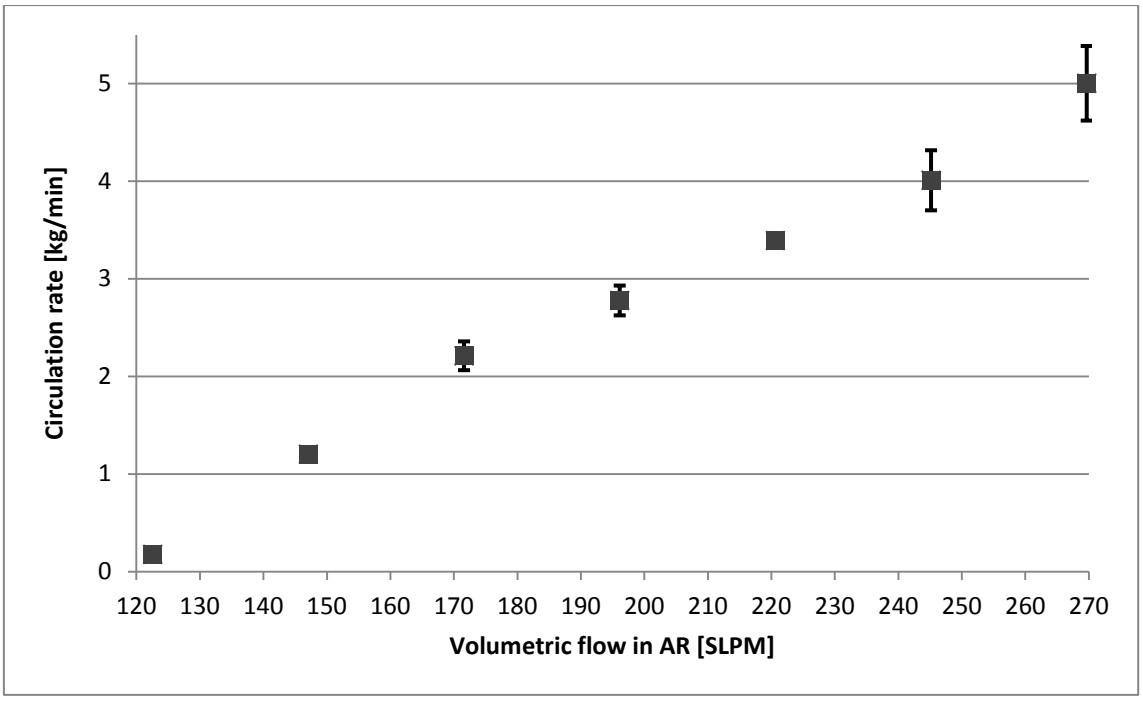

Figure 15. The circulation rate as a function of the volumetric flow in the AR when there is 7.31 kg (16.1 lbs) of particles in it. The dependency seems to be linear and the maximum circulation rate was measured to around 5 kg/min (11.0 lbs/min).

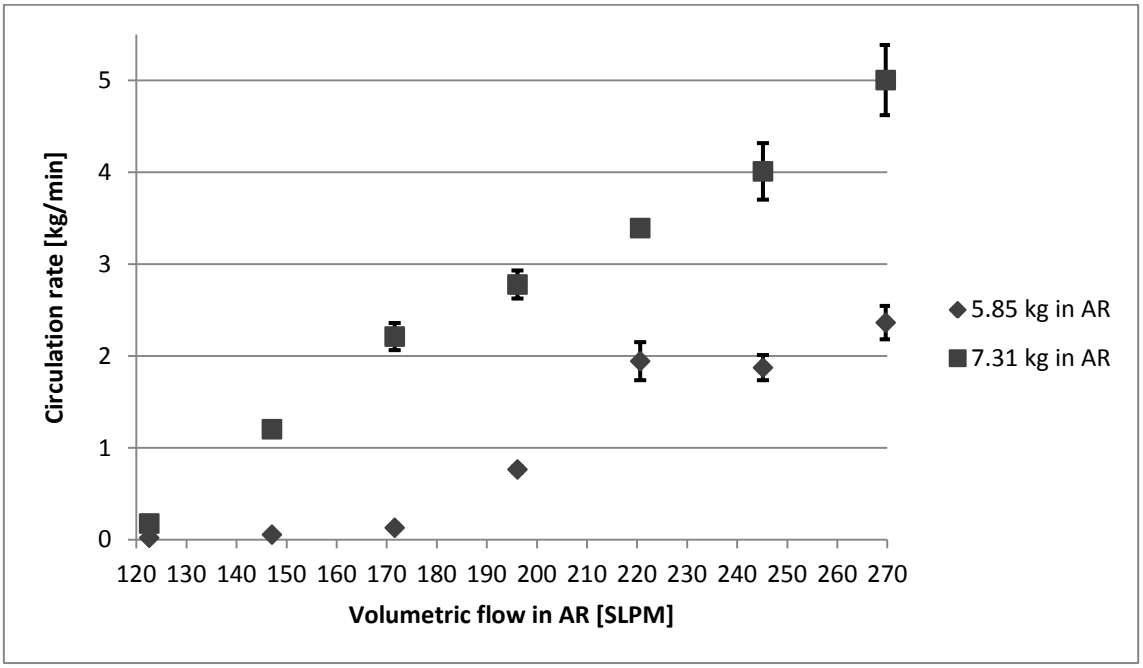

Figure 16. The circulation rate as a function of the volumetric flow in the AR for the two cases when having 5.85 kg (12.9 lbs) and 7.31 kg (16.1 lbs) in the AR respectively. The circulation rate is higher when there are more particles in the bed.

It may seem strange that one of the cases shows non-linear dependency whilst the other seem to be linear but this might be because it is first at lower circulation rates that the non-linear case seem to level out. Compare, for example, the point for the 5.85 kg case at around 170 SLPM to the point at around 120 SLPM for the case with 7.31 kg in the bed. These two cases have almost the same circulation rate but for the case with 5.85 kg two lower flows are examined as well and they have similar circulation rate as the one

at around 170 SLPM. If lower volumetric flows would have been tried for the case with 7.31 kg in the bed the same thing might have been observed.

How the circulation rate is dependent on the flow through the FR was finally examined and the result can be seen in Figure 17. It seems to be increasing and then stabilizing around a circulation rate of 1.4 kg/min (3.09 lbs/min). This may be the result of that the bed in the FR starts to bubble more violently and create larger bubbles at higher velocities making more particles fall over the edge and down the middle tube. This would have the same effect as increasing the amount of particles in the AR since there is not as much particles in the FR and instead they end up in the AR. Increasing the amount of particles in the AR also increases the circulation rate according to Figure 16 and this may be the reason for why the circulation rate increases with increasing flow through the FR. This does not on the other hand explain why it stabilizes at higher flows. It might stabilize due to the fact that at higher velocities the particles tend to continue upwards rather than distribute across the bed. These particles being thrown up from the bed will drop back down to the bed and some might fall down the middle tube but many will go straight back to the bed. This would result in some sort of internal circulation in the FR with particles being thrown up from it and later on returning to the same again rather than dropping down the middle tube.

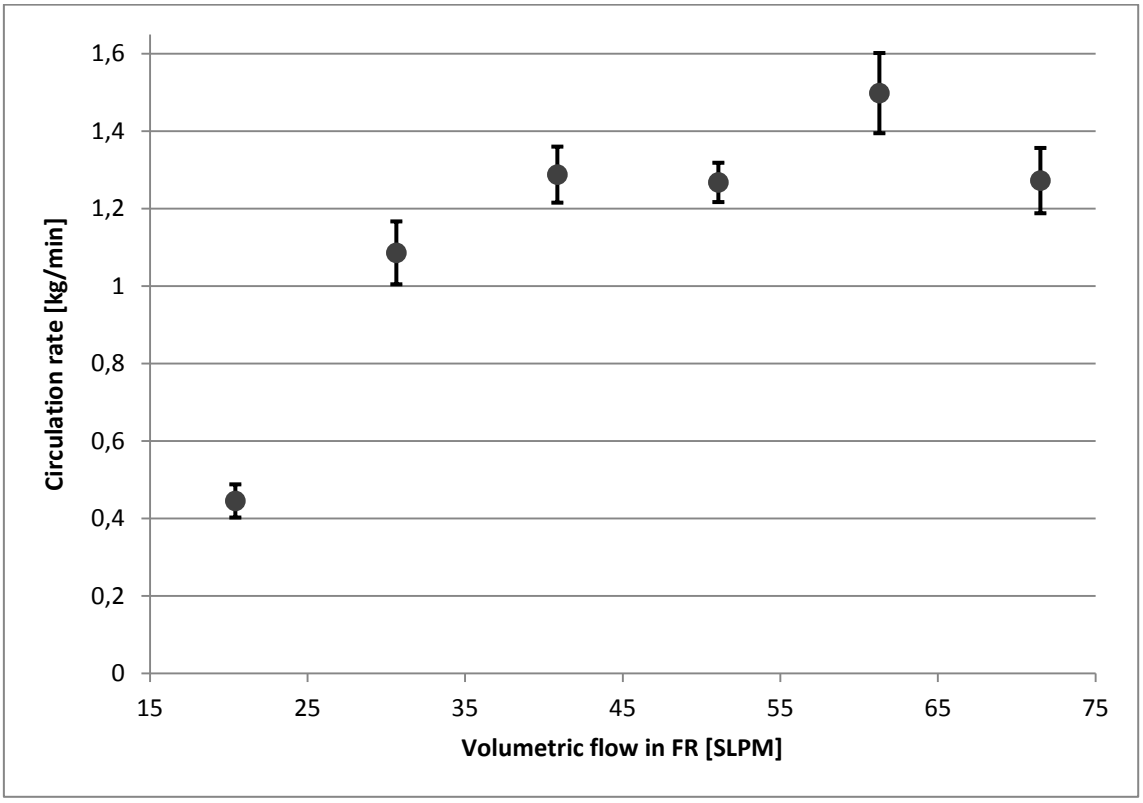

Figure 17. The circulation rate as a function of the volumetric flow in the FR when there is 7.31 kg (16.1 lbs) of particles in the AR. The flow through the AR was set to 147 SLPM (312 SCFH).

8. Conclusion

The aim was to design and build a chemical looping system, establish circulation and measure the circulation rate. The system got built and circulation was established after an extra jet was inserted at both the inlets of the fuel reactor and air reactor to force the particles into the reactors. The distance between the cyclone and the upper loop seal had to be increased by 518 mm (20.4") from the original design due to build-up of particles into the cyclone. The circulation rate was seen to be dependent on the amount of particles in the AR, the flow rate in the AR as well as the flow rate in the FR. An increased amount of particles lead to increased circulation and an increase of flow through the AR resulted in higher circulation. Finally also an increased flow in the FR increased the circulation rate until it stabilized around 1.4 kg/min (3.09 lbs/min). The maximum circulation rate observed was around 5 kg/min (11.0 lbs/min).

References

[1] Solomon, S. Plattner, G-K. Knutti, R. Friedlingstein, P. (2009) Irreversible climate change due to carbon dioxide emissions. *Proceedings of the National Academy of Sciences of the United States of America*, vol. 106, no 6, pp. 1704-1709.

[2] Orth, M. Ströhle, J. Epple, B. (2012) Design and Operation of a 1 MW_{th} Chemical Looping Plant. *2nd International Conference on Chemical Looping*; 26-28 September, 2012, Darmstadt.

[3] Herzog, H. Golomb, D. (2004) Carbon Capture and Storage from Fossil Fuel Use. *Encyclopedia of Energy*, vol. 1, pp. 277-287.

[4] Cao, Y. Sit, S.P. Pan, W.-P. (2012) The development of 10-KW Chemical Looping Combustion Technology in ICSET, WKU. *2nd International Conference on Chemical Looping*; 26-28 September, 2012, Darmstadt.

[5] Leion, H. Mattisson, T. Lyngfelt, A. (2007) The use of petroleum coke as fuel in chemical-looping combustion. *Fuel*, vol. 86, no 12-13, pp. 1947-1958.

[6] Johansson, E. Mattison, T. Lyngfeldt, A. Thunman, H. (2006) Combustion of Syngas and Natural Gas in a 300 W Chemical-Looping Combustor. *Chemical Engineering Research and Design*, vol. 84, no 9, pp. 819-827.

[7] Jerndal, E. Mattisson, T. Lyngfeldt, A. (2006) Thermal Analysis of Chemical-Looping Combustion. *Chemical Engineering Research and Design*, vol. 84, no 9, pp. 795-806.

[8] Rydén, M. Leion, H. Mattisson, T. Lyngfelt, A. (2014) Combined oxides as oxygen-carrier material for chemical-looping with oxygen uncoupling. *Applied Energy*, vol. 113, pp. 1924-1932.

[9] Leion, H. Mattisson, T. Lyngfelt, A. (2009) Using chemical-looping with oxygen uncoupling (CLOU) for combustion of six different solid fuels. *Energy Procedia*, vol. 1, pp. 447-453.

[10] Mattisson, T. Lyngfelt, A. Leion, H. (2009) Chemical-looping with oxygen uncoupling for combustion of solid fuels. *International Journal of Greenhouse Gas Control*, vol. 3, pp. 11-19.

[11] Gayán, P. Adánez-Rubio, I. Abad, A. de Diego, L.F. García-Labiano, F. Adánez, J. (2012) Development of Cu-based oxygen carriers for Chemical-Looping with Oxygen Uncoupling (CLOU) process. *Fuel*, vol. 96, pp. 226-238.

[12] Basu, P. Butler, J. (2009) Studies on the operation of a loop-seal in circulating fluidized bed boilers. *Applied Energy*, vol. 86, no. 9, pp. 1723-1731.

[13] Kunii, D. Levenspiel, O.(1991) Introduction. *Fluidization Engineering*, editor H. Brenner, pp. 1-13. Newton: Butterworth-Heinemann.

[14] Basu, P.(2006) Hydrodynamics. *Combustion and Gasification in Fluidized Beds*, pp. 21-58. Boca-Raton: Travis & Francis Group.

[15] Kunii, D. Levenspiel, O.(1991) Fluidization and Mapping of Regimes. *Fluidization Engineering*, editor H. Brenner, pp. 61-94. Newton: Butterworth-Heinemann.

[16] Rubel, A. Liu, K. Neathery, J. Taulbee, D. (2009) Oxygen carriers for chemical looping combustion of solid fuels. *Fuel*, vol. 88, no. 5, pp. 876-884.

[17] Adánez, J. de Diego, L.F. García-Labiano, F. Gayán, P. Abad, A. (2004) Selection of Oxygen Carriers for Chemical-Looping Combustion. *Energy & Fuels*, vol. 18, pp. 371-377.

[18] Cuadrat, A. Abad, A. Adánez, J. de Diego, L.F. García-Labiano, F. Gayán, P. (2012) Behavior of ilmenite as oxygen carrier in chemical-looping combustion. *Fuel Processing Technology*, vol. 94, no. 1, pp. 101-112.

[19] Lyngfeldt, A. (2011) Oxygen Carriers for Chemical Looping Combustion - 4 000 h of Operational Experience. *Oil & Gas Science and Technology - Rev. IFP Energies nouvelles*, vol. 94, no. 2, pp. 161-172.

[20] Adanez, J. Abad, A. García-Labiano, F. Gayán, P. de Diego, L.F. (2012) Progress in Chemical-Looping Combustion and Reforming technologies. *Progress in Energy and Combustion Science*, vol. 38, no. 2, pp. 215-282.

[21] Sozinho, T. Pelletant, W. Stainton, H. Guillou, F. Gauthier, T. (2012) Main results of the 10 kW_{th} pilot plant operation. *2nd International Conference on Chemical Looping*; 26-28 September, 2012, Darmstadt.

[22] Thon, A. Kramp, M. Hartge, E.-U. Heinrich, S. Werther, J. (2012) Operational experience with a coupled bed system for Chemical Looping Combustion of solid fuels. *2nd International Conference on Chemical Looping*; 26-28 September, 2012, Darmstadt.

[23] Sit, S.P. Reed, A. Hohenwarter, U. Horn, V. Marx, K. Pröll, T. (2012) 10 MW CLC Field Pilot. *2nd International Conference on Chemical Looping*; 26-28 September, 2012, Darmstadt.

[24] University of Utah. The Institute for Clean and Secure Energy, http://www.icse.utah.edu/leftnavid3subleftnavid9subpage1 (retrieved 2014-04-11).

[25] Sarofim, A. F. Lighty, J.S. Smith, P. J. Whitty, K. J. Eyring, E. Sahir, A. Alvarez, M. Hradisky, M. Clayton, C. Konya, G. Baracki, R. Kelly, K. (2011) *Chemical Looping Combustion Reactions and Systems*. Salt Lake City. (Task 5 Topical Report, Utah Clean Coal Program).

[26] Hamilton, M. A. Lighty, J. S. (2013) Modelling of a Scaled 300 kW_{th} Circulating Fluidized Bed Reactor with Barracuda. *2013 AlChe Annual Meeting*. November 3-8, 2013, San Francisco.

[27] Rubel, A. Liu, K. Neathery, J. Taulbee, D. (2009) Oxygen carriers for chemical looping combustion of solid fuels. *Fuel*, vol. 88, no. 5, pp. 876-884.

[28] North Carolina State University. Li Research Group, Sustainable Energy Research Lab, http://www.che.ncsu.edu/ligroup/index-lfx.html# (retrieved 2014-04-11).

[29] University of Connecticut. Process Design Simulation & Optimization Laboratory, http://pdsol.engr.uconn.edu/research2.html (retrieved 2014-04-11).

[30] Bayham, S. C. Kim, H. R. Wang, D. Tong, A. Zeng, L. McGiveron, O. Kathe, M. V. Chung, E. Wang, W. Wang, A. Majumder, A. Fan, L.-S. (2013) Iron-Based Coal Direct Chemical Looping Combustion Process: 200-h Continuous Operation of a 25-kW_{th} Subpilot Unit. *Energy Fuels*, vol. 27, no. 3, pp. 1347-1356.

[31] Tong, A. Bayham, S. Kathe, M. V. Zeng, L. Luo, S. Fan, L.-S. (2014) Iron-based syngas chemical looping process and coal-direct chemical looping process development at Ohio State University. *Applied Energy*, vol. 113, pp. 1836-1845.

[32] Siefert, N. S. Shekhawat, D. Litster, D. Berry, D. A. (2013) Steam-Coal Gasification Using CaO and KOH for *in Situ* Carbon and Sulfur Capture. *Energy & Fuels*, vol. 27, no. 8, pp. 4278-4289.

[33] Christensen, B. (2011) *Design and Performance of a Bench-Scale Steam Fluidized Gasifier for Biomass Analysis*. Salt Lake City: University of Utah. (Master Thesis at the department of Chemical Engineering).

[34] Basu, P.(2006) Air Distribution Grate. *Combustion and Gasification in Fluidized Beds*, pp. 359-380. Boca-Raton: Travis & Francis Group.

[35] Basu, P. Fraser, S. A. (1991) Design of CFB Components. *Circulating Fluidized Bed Boilers - Design and Operations*, pp. 229-250. Stoneham: Butterworth-Heinemann.

Appendix A

In this appendix drawings of the entire system, fuel reactor, air reactor, loop seals and cyclone are presented with dimensions in inches since SolidWorks used United States customary units.

Complete system

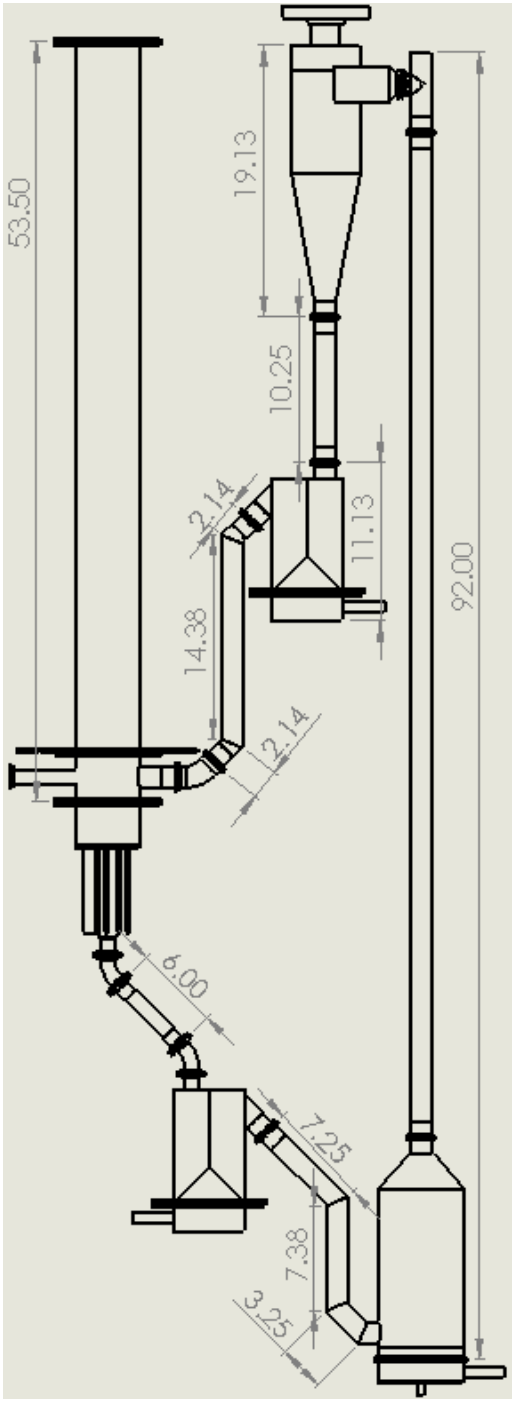

Figure A1. The complete system with some of the major parts. The dimensions for the AR riser and the tube connecting the cyclone to the upper loop seal is before 518 mm (20.4'') was added.

Fuel reactor

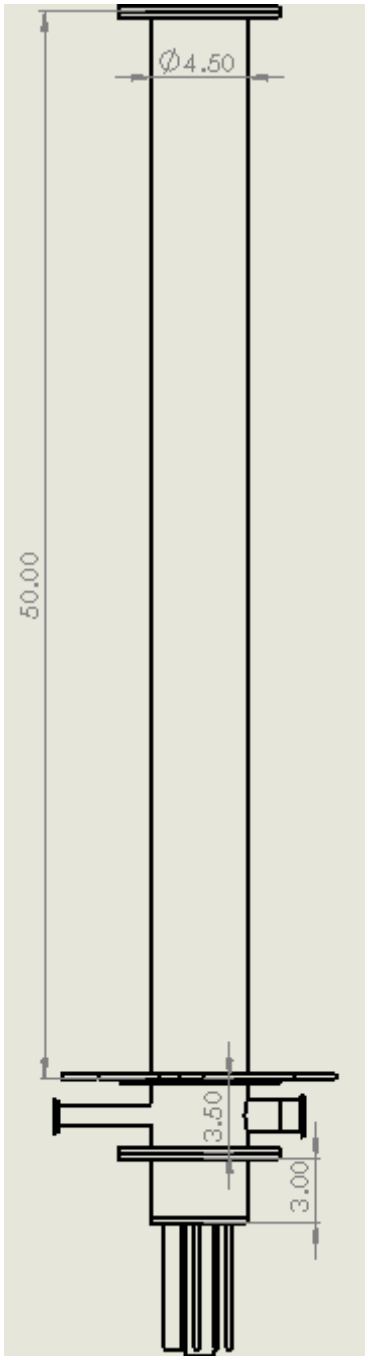

Figure A2. The complete fuel reactor where the pipe coming in from the left is the solid fuel feed and the pipe from the right is the particle inlet. The small pipes at the bottom of the fuel reactor are inlet pipes for thermocouples, a drain pipe and the outlet tube going on to the loop seal and later on to the air reactor. The pipe sticking up through the middle tube is tall enough to ensure a bed height of 154 mm (10'').

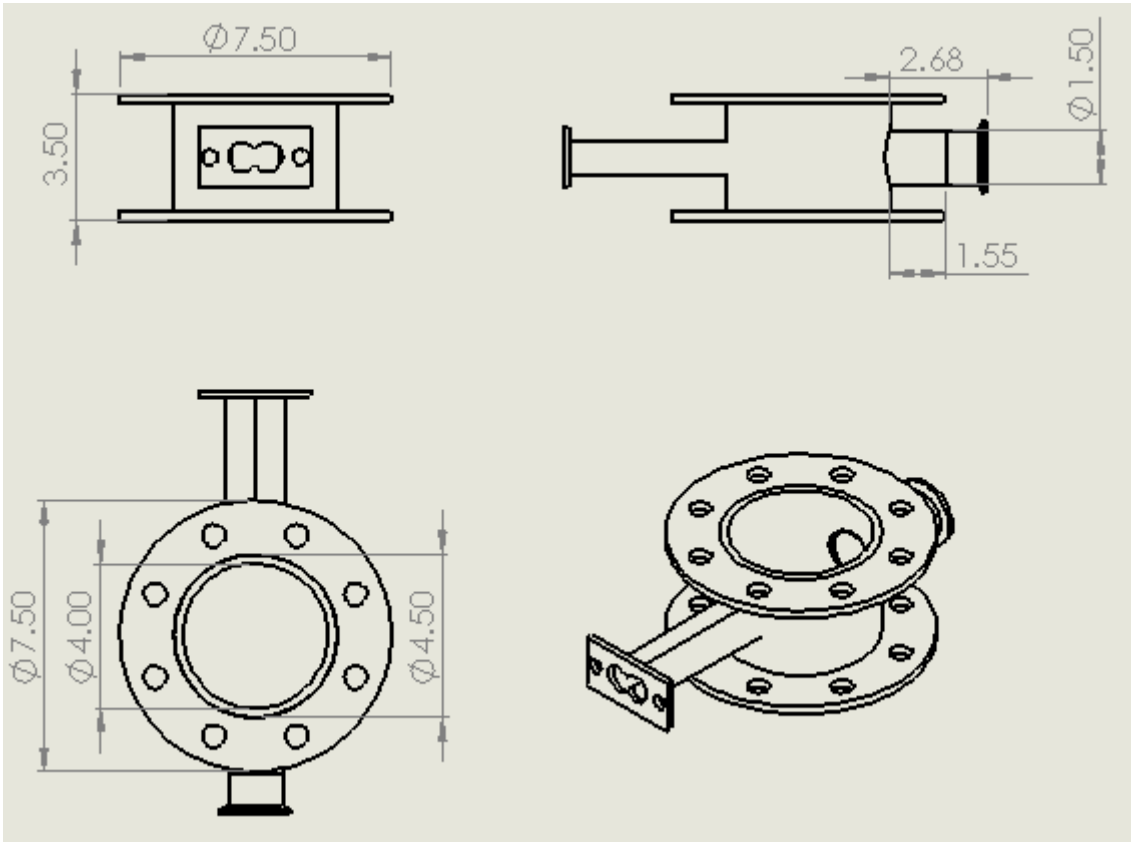

Figure A3. The additional piece added to the old gasifier. The inlet of the solid fuel has the shape of a two pipes welded together since it consists of two screws pushing the fuel into the reactor.

Air reactor

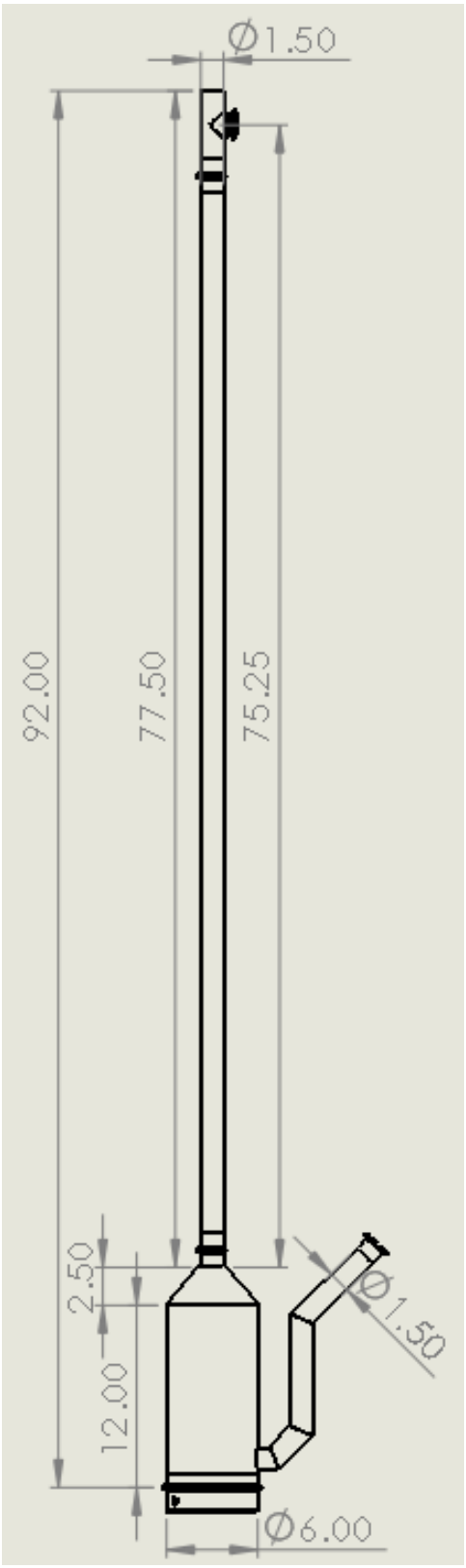

Figure A4. The entire air reactor. The plenum is also added at the bottom of the reactor and consists of a shallow bowl with the distributor plate on top. Note that the dimension for the riser is before 518 mm (20.4'') was added.

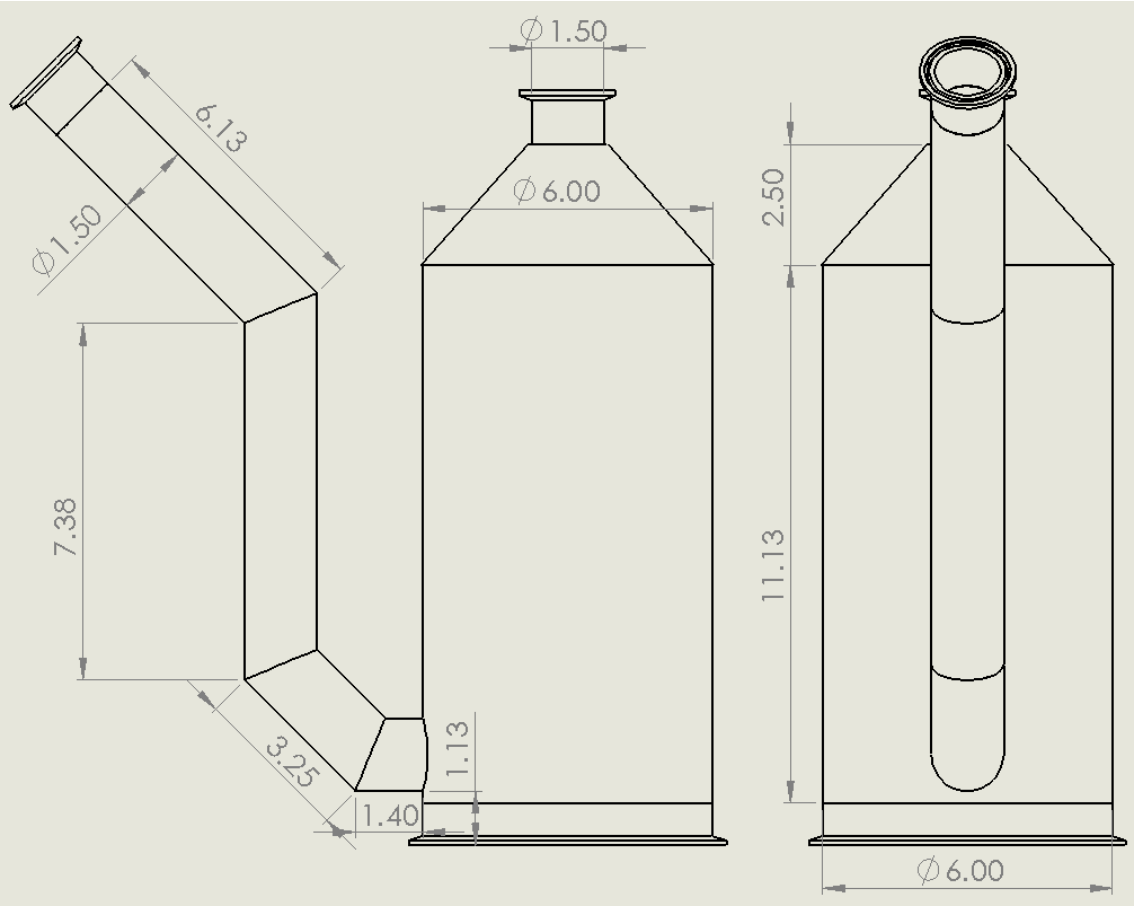

Figure A5. The bottom part of the air reactor in which a bubbling bed is desired.

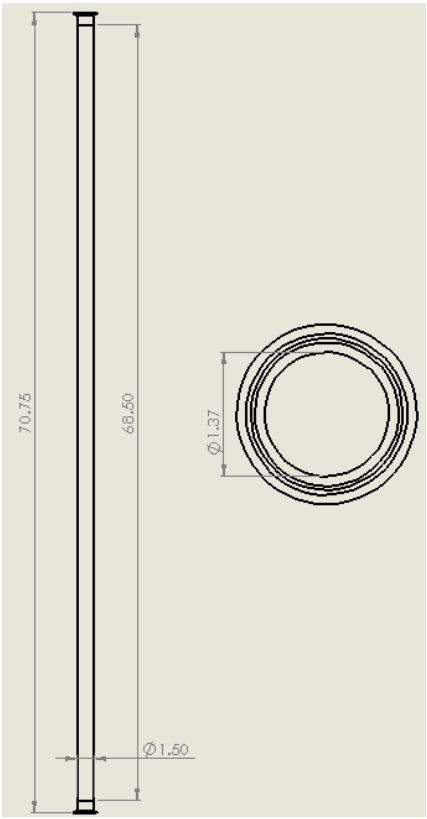

Figure A6. The riser of the air reactor which consists of a long pipe. A transport bed is desired in this part. Note that the height of the riser is before 518 mm (20.4'') was added.

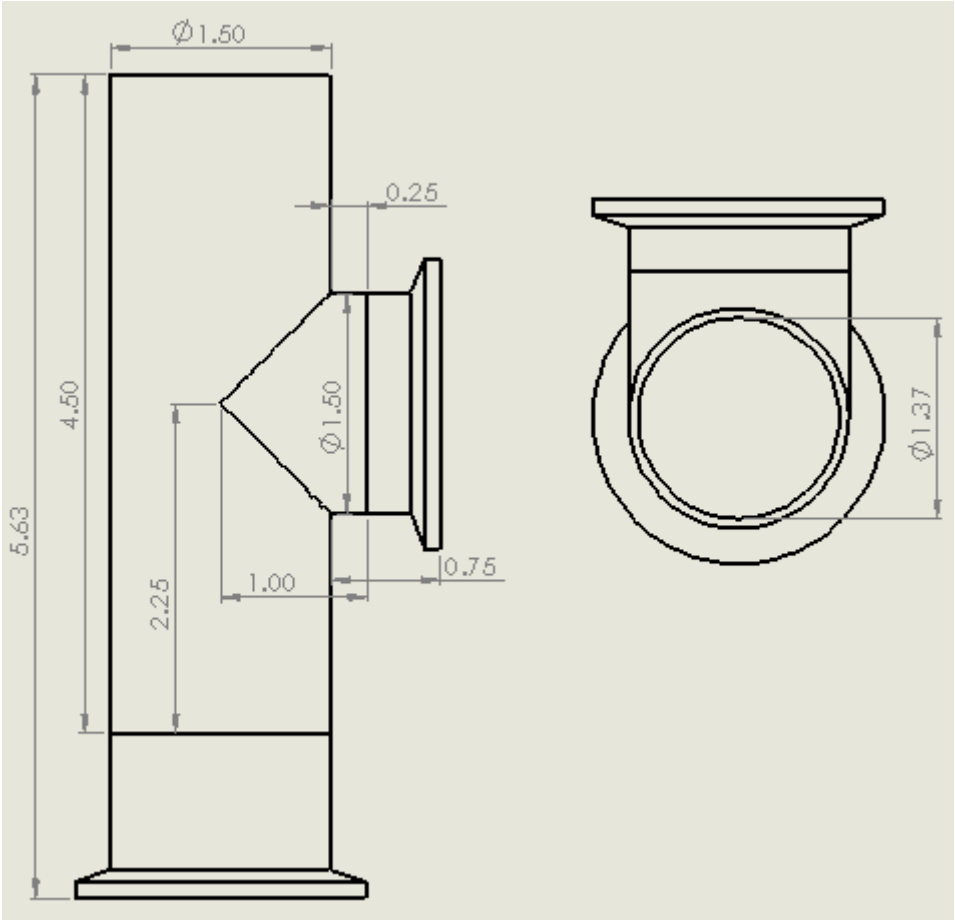

Figure A7. The top piece of the air reactor which goes off to the cyclone.

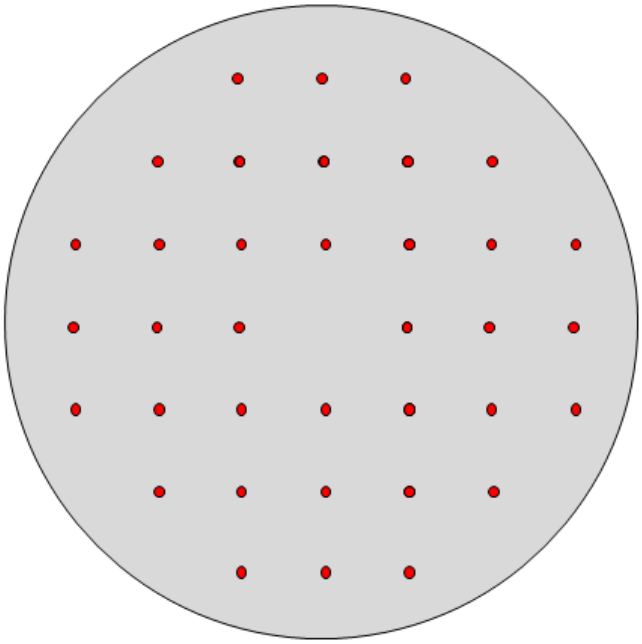

Figure A8. The hole pattern for the air reactor distributor plate. Each hole is 1.59 mm (0.0625") in diameter.

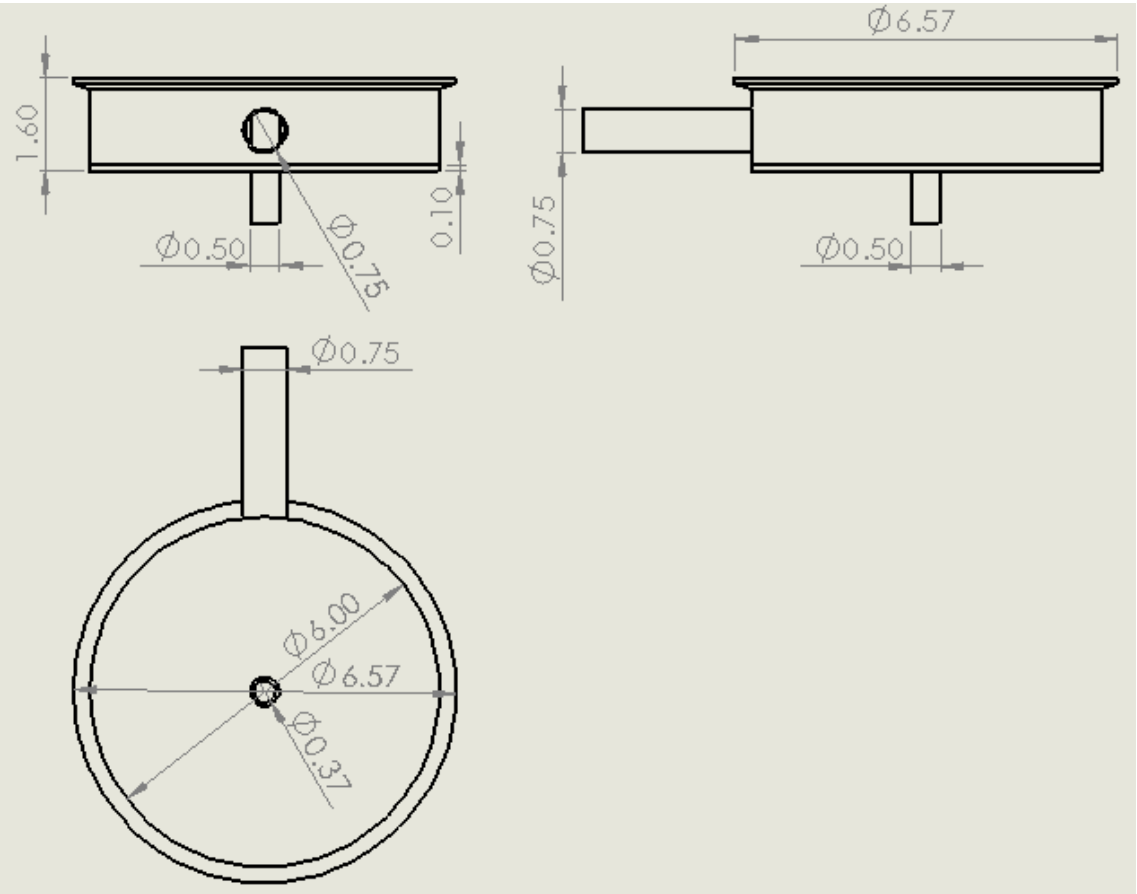

Figure A9. The air reactor plenum with the air inlet from the side and a particle drain in the bottom.

Loop seals

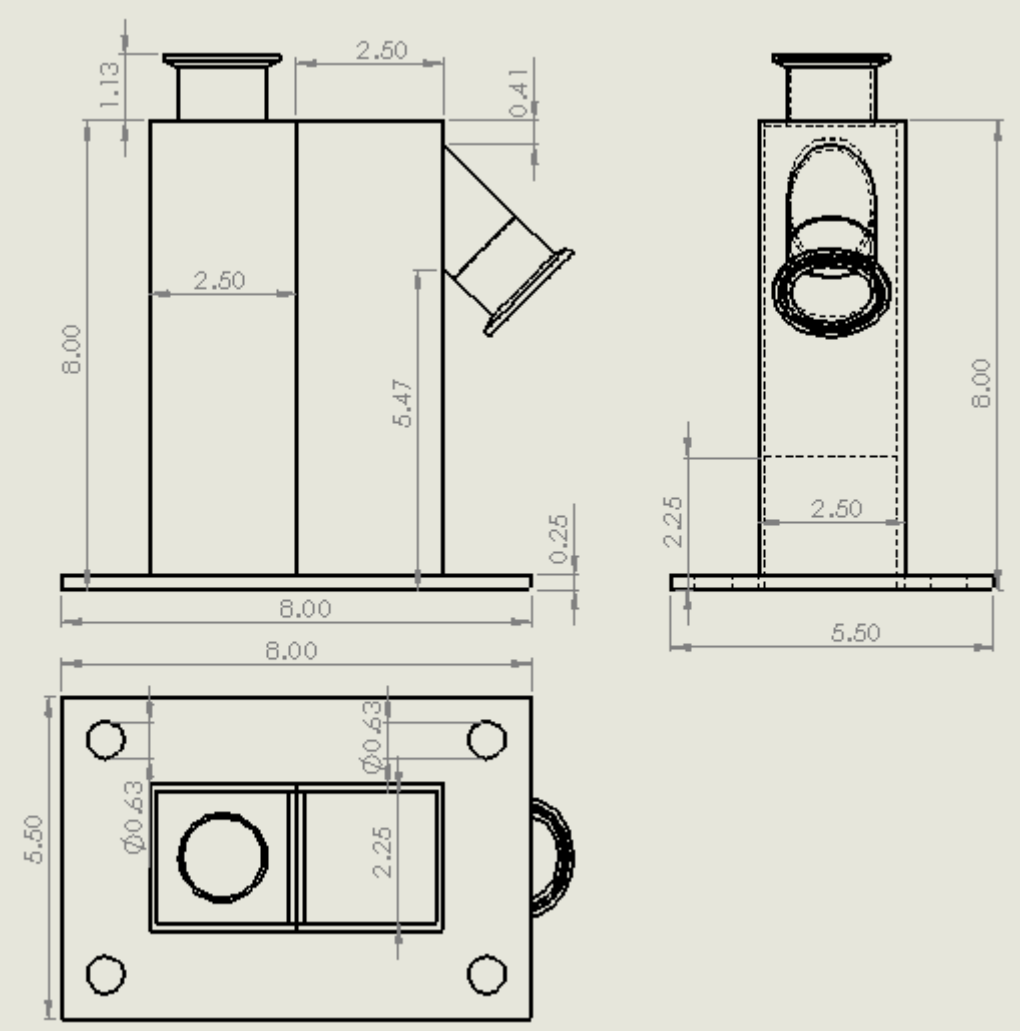

Figure A10. The loop seal design which consists of two square tubes welded together.

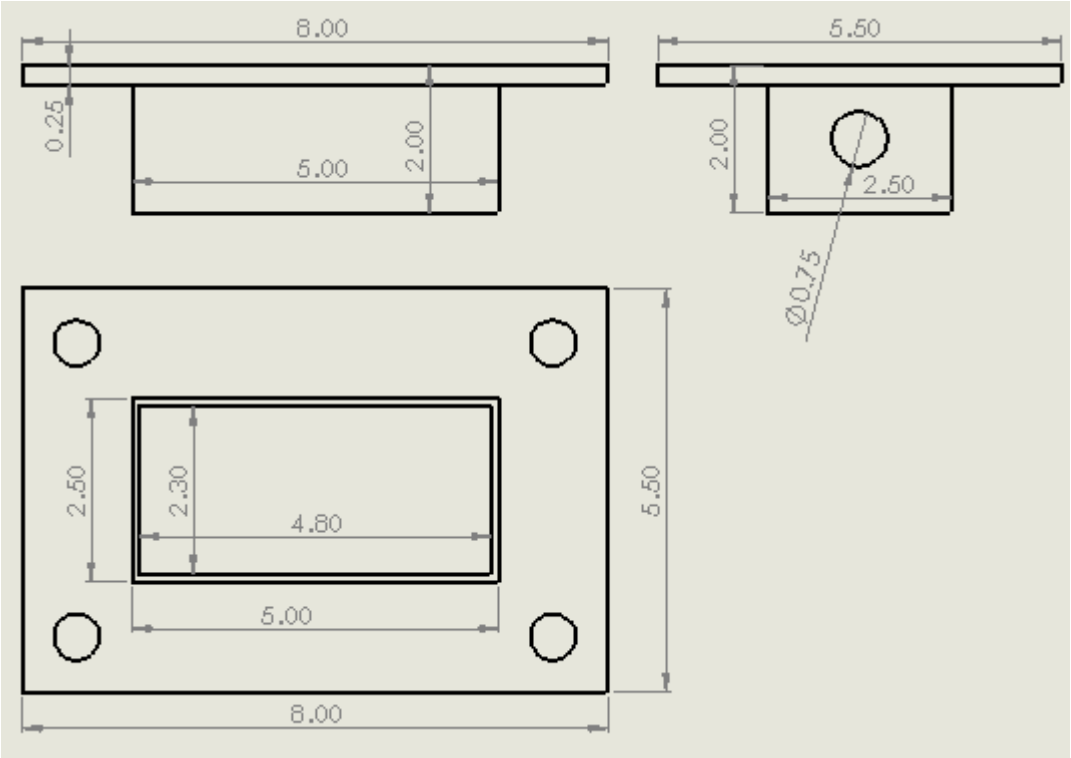

Figure A11. The loop seal plenum with the gas inlet on the side.

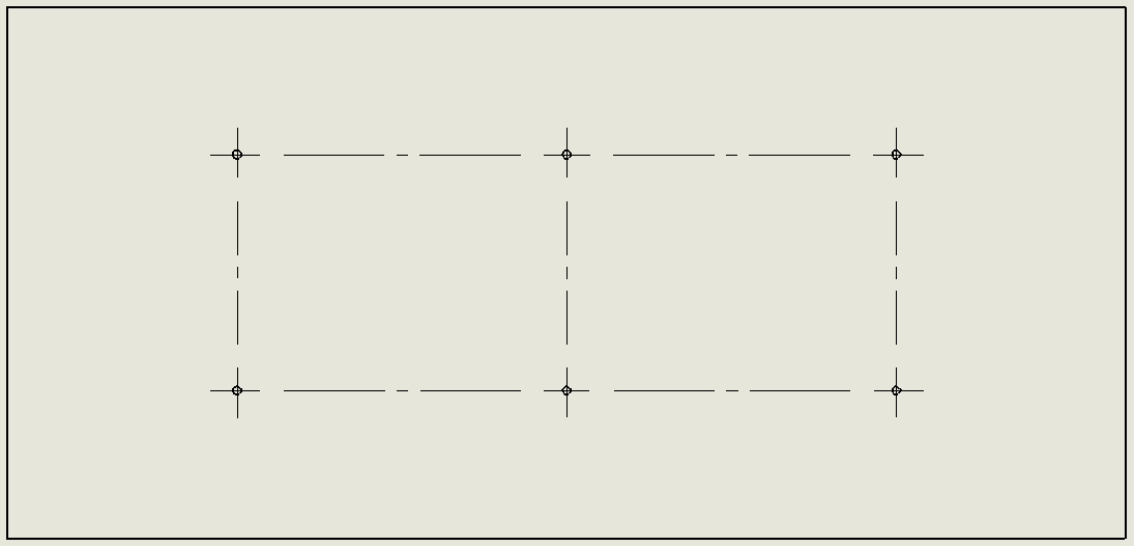

Figure A12. The loop seal distributor plate hole pattern.

Cyclone

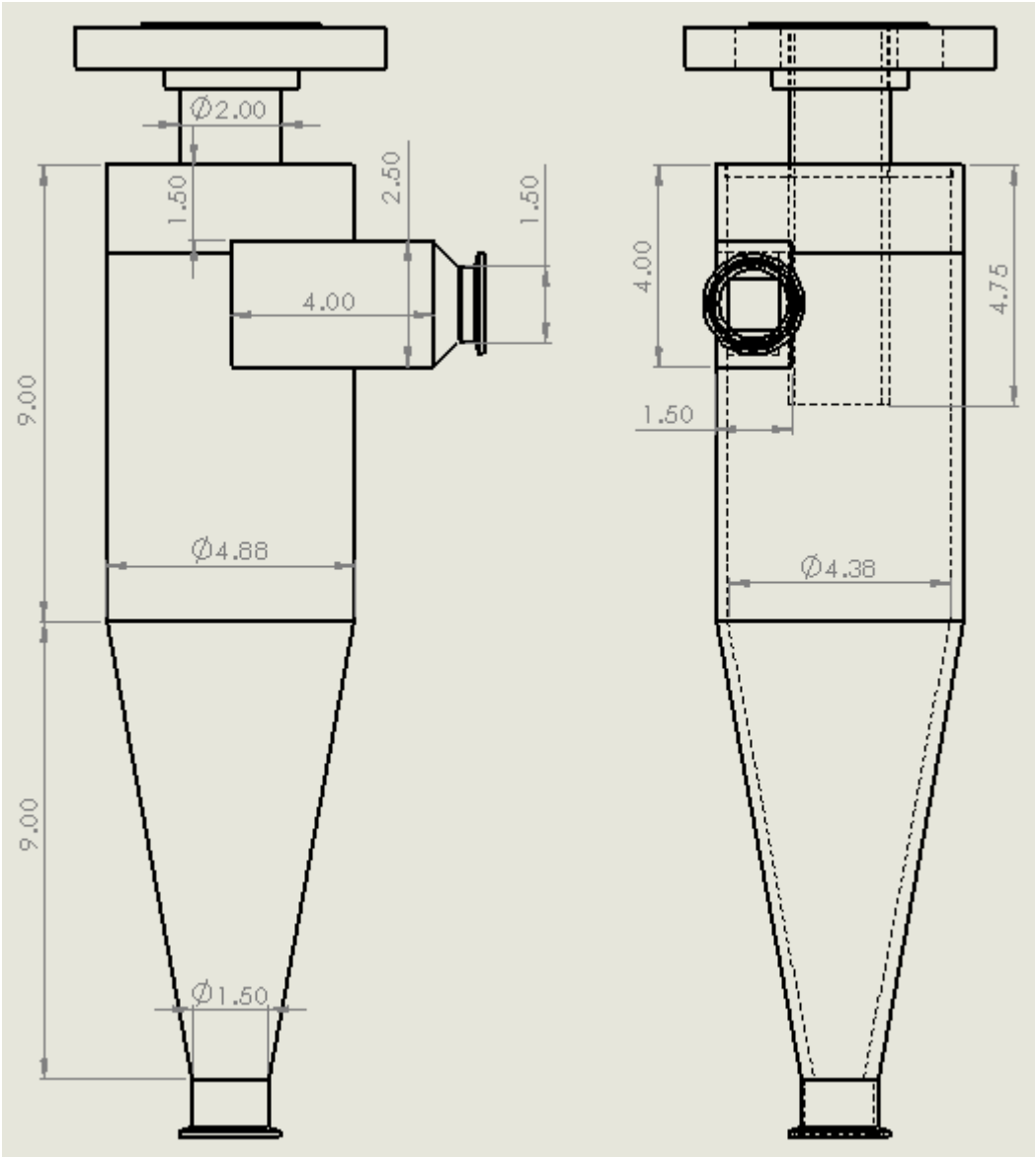

Figure A13. The dimensions of the reused cyclone.

Appendix B

Table B1. Listing all different tubes used for the system. The place from which the material was bought is included as well as their product number whenever known.

Part	Material	Dimensions	From	Product number
Tube	304 Stainless steel	ID = 147 mm (5.78') OD = 152 mm (6")	Rolled from metal sheet	
Tube	321 Stainless steel	ID = 102 mm (4") OD = 114 mm (4.5")		
Tube	304 Stainless steel	ID = 38.1 mm (1.37") OD = 38.1 mm (1.5")	McMASTER-CARR	8989K858
Tube	304 Stainless steel	ID = 22.1 mm (0.87") OD = 25.4 mm (1")	McMASTER-CARR	8989K848
Square tube	304 Stainless steel	IL = 57.2 mm (2.25") OL = 63.5 mm (2.5")		

Table B2. All different types of quick-clamp connectors used and the clamps used for the connections.

Part	Material	Dimensions	From	Product number
Quick-clamp connector	304 Stainless steel	ID = 147 mm (5.78") OD = 152 mm (6") L = 38.1 mm (1.5")	McMASTER-CARR	4322K167
Quick-clamp connector	304 Stainless steel	ID = 147 mm (5.78") OD = 152 mm (6") L = 22.2 mm (0.875")	McMASTER-CARR	4322K217
Quick-clamp connector	304 Stainless steel	ID = 38.1 mm (1.37") OD = 38.1 mm (1.5") L = 28.6 mm (1.125")	McMASTER-CARR	4322K162
Quick-clamp connector	304 Stainless steel	ID = 38.1 mm (1.37") OD = 38.1 mm (1.5") L =12.7 mm (0.5")	McMASTER-CARR	4322K212
Quick-clamp connector	304 Stainless steel	ID = 23.7 mm (0.932") OD = 25.4 mm (1") L = 28.6 mm (1.125")	McMASTER-CARR	4322K161
Quick-clamp clamp	304 Stainless steel	For 6" connector	McMASTER-CARR	4322K157
Quick-clamp clamp	304 Stainless steel	For 1" and 1.5" connector	McMASTER-CARR	4322K152